

AD-A038 759

NAVAL POSTGRADUATE SCHOOL MONTEREY CALIF F/G
THE FINITE ELEMENT METHOD APPLIED TO FLOWS IN TURBOMACHINES. (U)
DEC 76 V F GAVITO

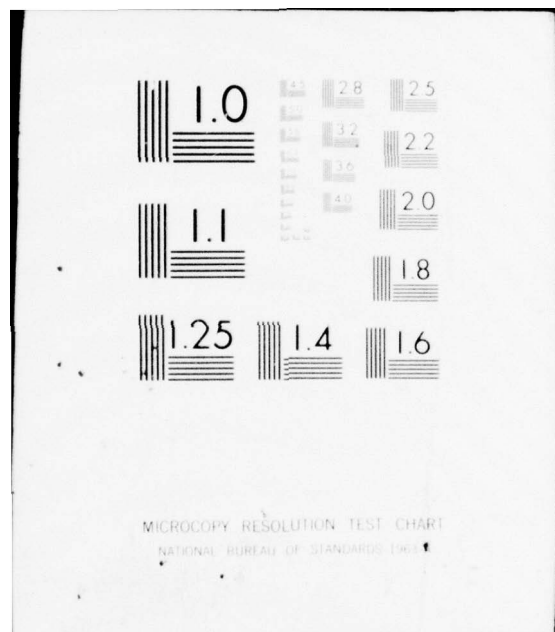
F/6 20/4

UNCLASSIFIED

NL

1 OF 2
AD
A038759





AD A 038759

P
NAVAL POSTGRADUATE SCHOOL
Monterey, California



THESIS

THE FINITE ELEMENT METHOD APPLIED TO FLOWS IN
TURBOMACHINES

by

Valentin Francisco Gavito, Jr.

December 1976

Thesis Advisor:

D.J. Collins

Approved for public release; distribution unlimited.

AD No.
DDC FILE COPY

REPORT DOCUMENTATION PAGE		READ INSTRUCTIONS BEFORE COMPLETING FORM
1. REPORT NUMBER	2. GOVT ACCESSION NO.	3. RECIPIENT'S CATALOG NUMBER
4. TITLE (and Subtitle) 6 The Finite Element Method Applied To Flows In Turbomachines		5. TYPE OF REPORT & PERIOD COVERED 7 Master's Thesis, December 1976
7. AUTHOR(s) 10 Valentin Francisco Gavito, Jr		6. PERFORMING ORG. REPORT NUMBER
9. PERFORMING ORGANIZATION NAME AND ADDRESS Naval Postgraduate School Monterey, California 93940		8. CONTRACT OR GRANT NUMBER(s)
11. CONTROLLING OFFICE NAME AND ADDRESS Naval Postgraduate School Monterey, California 93940		10. PROGRAM ELEMENT, PROJECT, TASK AREA & WORK UNIT NUMBERS
14. MONITORING AGENCY NAME & ADDRESS (if different from Controlling Office)		12. REPORT DATE 11 December 1976
		13. NUMBER OF PAGES 12 125 p.
		18. SECURITY CLASS. (of this report) Unclassified
		18a. DECLASSIFICATION/DOWNGRADING SCHEDULE
16. DISTRIBUTION STATEMENT (of this Report) Approved for public release; distribution unlimited.		
17. DISTRIBUTION STATEMENT (of the abstract entered in Block 20, if different from Report)		
18. SUPPLEMENTARY NOTES		
19. KEY WORDS (Continue on reverse side if necessary and identify by block number) Finite Element Method Turbomachines		
20. ABSTRACT (Continue on reverse side if necessary and identify by block number) The finite element method is applied to the two-dimensional, inviscid, compressible radial equilibrium equation for axial compressors. Isoparametric elements are used along with three-point Gaussian integration for stiffness matrix evaluation. The radial equilibrium equation is put into quasi-harmonic form for stream function formulation and results are presented using an isentropic flow assumption. Axial velocity profiles at rotor and stator blade edges are compared with published performance data		

251450

of the NASA Task-1 stage transonic compressor and with numerical finite element results of Hirsch and Warzee.

ACCESSION FOR	
NTIS	Write Section <input checked="" type="checkbox"/>
DOC	Buff Section <input type="checkbox"/>
UNANNOUNCED	
JUSTIFICATION	
BY DISTRIBUTION/AVAILABILITY CODES	
DISC.	ASAC. DISC. SPECIAL
<i>H</i>	

THE FINITE ELEMENT METHOD APPLIED TO FLOWS IN
TURBOMACHINES

by

Valentin Francisco Gavito, Jr.
Lieutenant, United States Navy
B.S.M.E., Southern Methodist University, 1970

Submitted in partial fulfillment of the
requirements for the degree of

MASTER OF SCIENCE IN AERONAUTICAL ENGINEERING

from the
NAVAL POSTGRADUATE SCHOOL
December 1976

Author:

Valentin Francisco Gavito, Jr.

Approved by:

Daniel J. Collins

Thesis Advisor

Raymond A. Shoenue

Second Reader

Richard W. Bell

Chairman, Department of Aeronautics

Robert A. Johnson

Dean of Science and Engineering

ABSTRACT

The finite element method is applied to the two-dimensional, inviscid, compressible radial equilibrium equation for axial compressors. Isoparametric elements are used along with three-point Gaussian integration for stiffness matrix evaluation. The radial equilibrium equation is put into quasi-harmonic form for stream function formulation and results are presented using an isentropic flow assumption. Axial velocity profiles at rotor and stator blade edges are compared with published performance data of the NASA Task-1 stage transonic compressor and with numerical finite element results of Hirsch and Warzee.

TABLE OF CONTENTS

I.	INTRODUCTION.....	7
A.	PROBLEM STATEMENT AND OBJECTIVE.....	7
II.	THEORY.....	10
A.	THE DERIVATION OF THE RADIAL EQUILIBRIUM EQUATION.....	10
B.	THE FINITE ELEMENT METHOD APPLIED TO THE RADIAL EQUILIBRIUM EQUATION.....	20
C.	NUMERICAL INTEGRATION OF THE STIFFNESS MATRIX AND SOLUTION PROCEDURE.....	28
1.	Numerical integration of the stiffness matrix.....	28
2.	Solution procedure.....	32
a.	Discretization.....	32
b.	Initialization.....	32
c.	Calculation of thermodynamic variables.....	34
d.	Calculate matrices.....	37
e.	Solve system of equations.....	37
f.	Perform relaxation iteration.....	37
g.	Update velocity and density profiles.....	37
h.	Test for convergence of ψ	38
i.	Summary.....	38
III.	THE PROGRAM.....	40
A.	OVERALL FLOWCHART AND DESCRIPTION.....	40
B.	THE MAIN PROGRAM.....	43
1.	The input routine.....	43
a.	category 1.....	43
b.	category 2.....	43
c.	category 3.....	43
d.	category 4.....	43

e. category 5.....	43
f. category 6.....	44
g. category 7.....	44
h. category 8.....	44
i. category 9.....	44
j. category 10.....	44
k. category 11.....	44
l. category 12.....	44
2. Stiffness matrix evaluation.....	50
3. Solution of system of equations.....	52
4. Iteration schemes.....	52
5. The output routine.....	53
C. THE SUBROUTINES.....	53
1. Subroutine shape.....	54
2. Subroutine jacob.....	54
3. Subroutine sline.....	55
4. Subroutine fcal.....	58
5. Subroutine vel.....	61
6. Subroutine mplot.....	66
IV. TEST CASES AND RESULTS.....	67
V. CONCLUSIONS AND RECOMMENDATIONS FOR FURTHER STUDY.....	70
Appendix A: COMPUTER PROGRAM.....	76
Appendix B: SAMPLE INPUT DATA.....	100
Appendix C: SAMPLE OUTPUT LISTING.....	107
Appendix D: CALCULATION OF ROTOR ELEMENT FLOW ANGLES...	117
LIST OF FIGURES.....	122
LIST OF REFERENCES.....	123
INITIAL DISTRIBUTION LIST.....	125

I. INTRODUCTION

A. PROBLEM STATEMENT AND OBJECTIVE

The prediction of meridional flows within turbomachines, be they compressors or turbines, is a difficult but important part of the design process. The difficulty arises from the presence of three-dimensional and viscous effects within all turbomachines and the importance arises from the necessity to design accurately and efficiently.

To simplify the problem of viscous, three-dimensional analysis, Wu [Ref.1] showed that this complicated flow may be analyzed by solving two interrelated flows: one being the blade-to-blade flow describing the flow between rotating blades and the other being the meridional through flow which describes the radial equilibrium. These flows are depicted in Fig 1. In addition, an inviscid and axi symmetric assumption is made in the through-flow thereby simplifying the flow to a two-dimensional, axi symmetric, inviscid, and compressible analysis.

Three methods may be found in current reports regarding the solution of the radial equilibrium equation. The first two are the streamline curvature method [Ref.2,3,and 4] and the matrix method [Ref.5 and 6] which is basically a finite difference technique. The third, a relatively new method, is the finite element method. As shown by Hirsch and Warzee [Ref.7]', the solution of the radial equilibrium equation by the finite element method is achieved by arranging the

equation for the stream function in quasi-harmonic form.

Due to the excellent results reported in Ref.7 and to further the research effort for finite element techniques in fluid flow problems, the purpose of this thesis is two fold. Firstly, the goal was to formulate a computer program for solution of the radial equilibrium equation paralleling the steps as presented by Hirsch and Warzee. Secondly, after suitable verification of computer results with those of Hirsch and Warzee, the goal was to compare computer predicted flows with measured performance data of the Naval Post Graduate School's transonic compressor.

The purpose of this paper is to present a report on the results obtained thus far. In Section II, the derivation of the radial equilibrium equation is presented followed by the application of the finite element method to this equation. Section III describes the computer program in some detail. Section IV contains selected test cases which were used in program testing and checking. In Section V, conclusions are presented along with recommendations for further study and work on the project. The appendices contain the program listing along with a sample test case for reference by the user. In addition, a list of references is contained for further reading on the subject of this paper.

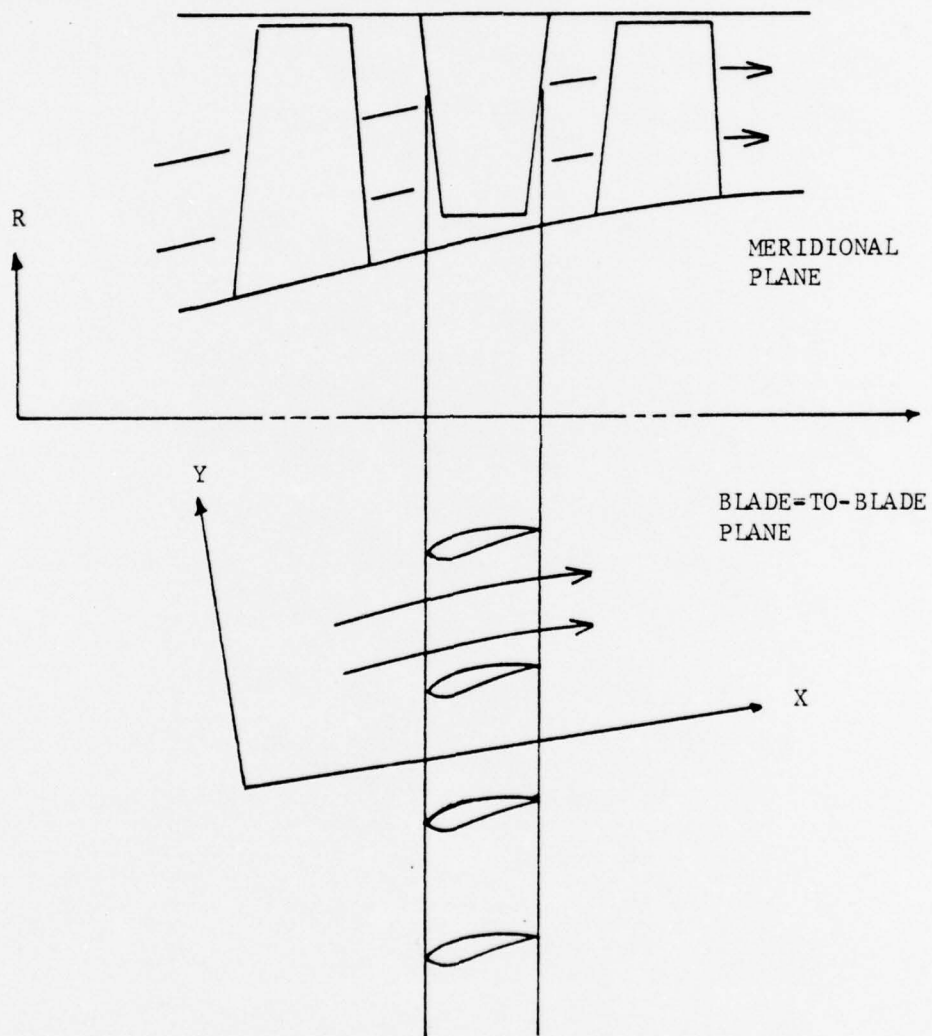


Figure 1 - MERIDIONAL AND BLADE-TO-BLADE PLANES

II. THEORY

A. THE DERIVATION OF THE RADIAL EQUILIBRIUM EQUATION

The following discussion is taken from Ref. 7 with slight changes in notation. The basic turbomachine geometry to be analyzed is depicted in Fig 2. Although the machine noted is one stage of a compressor, a similar analysis to the one that follows may be applied to other machines such as axial turbines and mixed-flow machines.

One begins with the Euler equation assuming the viscous forces to be negligible.

$$\frac{d\vec{V}}{dt} + (\vec{V} \cdot \nabla) \vec{V} = \nabla p / \rho \quad (\text{II.A.1})$$

The continuity equation, assuming unsteady flow is,

$$\frac{d\rho}{dt} + \nabla(\rho \vec{V}) = 0 \quad (\text{II.A.2})$$

The First Law of thermodynamics in a fluid field becomes,

$$T \nabla s = \nabla h - \nabla p / \rho \quad (\text{II.A.3})$$

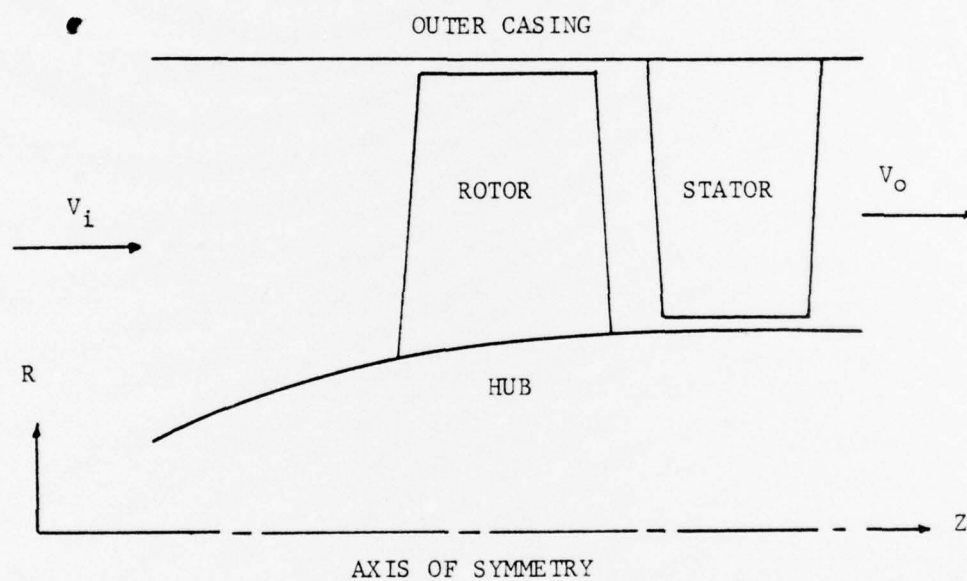


Figure 2 - TURBOMACHINE GEOMETRY

Substituting equation (II.A.3) into equation (II.A.1) leads to the Crocco equation,

$$\frac{d\vec{V}}{dt} - \vec{V} \times (\nabla \times \vec{V}) = T \nabla S - \nabla H \quad (\text{II.A.4})$$

where H is the total enthalpy.

Assuming a steady and adiabatic flow, the energy equation becomes simply,

$$(\vec{V} \cdot \nabla) H = 0 \quad (\text{II.A.5})$$

which shows that along a streamline in a stationary system, the total enthalpy is constant.

In a relative system, such as the case in a rotor blade row, the total relative velocity, \vec{W} , can be expressed in the following form,

$$\vec{W} = \vec{V} + \vec{\omega} \times \vec{R} = \vec{V} + \vec{U} \quad (\text{II.A.6})$$

where $\vec{\omega}$ is the constant angular velocity and \vec{U} is the constant peripheral speed of the relative system.

Now, the Crocco equation in a relative system becomes,

$$\frac{d\vec{W}}{dt} - \vec{W} \times (\nabla \times \vec{W}) = T \nabla S - \nabla \left(h + \frac{W^2}{2} - \frac{\omega^2 R^2}{2} \right) \quad (\text{II.A.7})$$

Parallel to equation (II.A.5) for the stationary system, the energy equation, assuming steady and adiabatic (relative) flow in a relative system, becomes

(II.A.8)

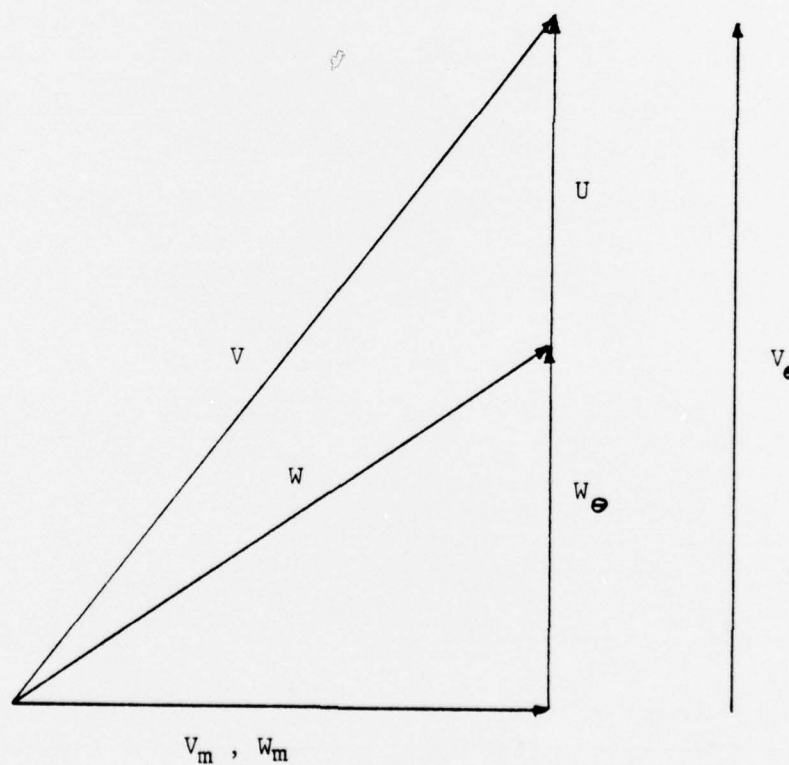
$$(\vec{w} \cdot \nabla) H_R = 0$$

where H_R is the relative total enthalpy expressed as follows,

(II.A.9)

$$H_R = h + \frac{w^2}{2} - \frac{\omega^2 R^2}{2}$$

From the following velocity diagram,



equation (II.A.9) may be arranged as follows.

Since,

$$W_m^2 + W_\theta^2 = W^2 = V_m^2 + (V_\theta - u)^2 \quad (\text{II.A.10})$$

then,

$$W^2 = V_m^2 + V_\theta^2 - 2uV_\theta + u^2 \quad (\text{II.A.11})$$

and,

$$W^2 = V^2 + u^2 - 2uV_\theta \quad (\text{II.A.12})$$

Substituting equation (II.A.12) into equation (II.A.9) leads to the following relation,

$$H_R = h + \frac{V^2}{2} - uV_\theta = H - uV_\theta \quad (\text{II.A.13})$$

Equation (II.A.8) shows that H_R is constant along a streamline in a relative system.

Upon integrating equation (II.A.8) between the rotor inlet and outlet, the Euler equation for turbomachines is found,

$$\Delta H \Big|_{IN}^{OUT} = \Delta (\vec{u} \cdot \vec{V}_\theta) \Big|_{IN}^{OUT} \quad (\text{II.A.14})$$

It may be shown [Ref.9] that by circumferentially averaging equation (II.A.1), and under the axi symmetric flow assumption the following relation is valid,

$$-\vec{V} \times (\nabla \times \vec{V}) = T \cdot \nabla S - \nabla H + F_b + F_d \quad (\text{II.A.15})$$

where F_b is the body force of the blades acting on the fluid and all variables are mean values along the direction of the circumference. Hence equation (II.A.15) is an approximation for axi symmetric flow. As a final note on equation (II.A.15), since the viscous forces were neglected in equation (II.A.1), there must be a force introducing the entropy variations along the blade. This force is proportional to the pressure loss coefficient and is labeled F_d , the dissipative force. F_d produces work which in turn produces entropy production radially along the blade. Under the axi symmetric assumption, entropy varies axially and radially only and is assumed to be proportional to the pressure loss coefficients [Ref. 2 and 8].

. Due to boundary conditions imposed on the problem and the axi symmetric assumption, cylindrical coordinates, (r, θ, z) , will be used in all subsequent analysis. Therefore, equation (II.A.15), in cylindrical coordinates and with axial symmetry is as follows,

$$\frac{V_\theta}{R} \frac{\partial}{\partial R} (R V_\theta) - V_z \left(\frac{\partial}{\partial z} V_r - \frac{\partial}{\partial R} V_z \right) = \frac{\partial H}{\partial R} - T \frac{\partial S}{\partial R} - F_{br} - F_{dr} \quad (\text{II.A.16})$$

$$\frac{V_z}{R} \frac{\partial}{\partial z} (R V_\theta) + \frac{V_r}{R} \frac{\partial}{\partial R} (R V_\theta) = F_\theta \quad (\text{II.A.17})$$

$$V_R \left(\frac{1}{R} \frac{\partial}{\partial z} V_R - \frac{\partial}{\partial R} V_z \right) - \frac{V_\theta}{R} \frac{\partial}{\partial z} (R V_\theta) = \frac{\partial H}{\partial z} - T \frac{\partial S}{\partial z} - F_z \quad (\text{II.A.18})$$

It is important to note here that under the axisymmetric assumptions, equation (II.A.15) reduces to the following,

$$\vec{V} \cdot \vec{F}_b = 0 \quad (\text{II.A.19})$$

Likewise in a relative system (rotor), the axisymmetric assumption leads to the following,

$$\vec{W} \cdot \vec{F}_b = 0 \quad (\text{II.A.20})$$

Equation (II.A.16) describes the meridional through flow radial equilibrium equation for the finite element method. Since one is concerned with the meridional plane, the following derivative expression is taken from Fig 3.

$$V_m \frac{\partial}{\partial m} = V_R \frac{\partial}{\partial R} + V_z \frac{\partial}{\partial z} \quad (\text{II.A.21})$$

Therefore equation (II.A.17) reduces to,

$$R F_\theta = V_m \frac{\partial}{\partial m} (R V_\theta) \quad (\text{II.A.22})$$

which reveals that in a duct where there are no blades and therefore no blade forces, angular momentum is constant

along a streamline. In that case,

$$\frac{d}{dm}(R V_\theta) = 0 \quad (\text{II.A.23})$$

As shown in Ref.9, the circumferentially averaged continuity equation is the following,

$$\frac{d}{dR}(\rho R b V_R) + \frac{d}{dz}(\rho R b V_z) = 0 \quad (\text{II.A.24})$$

where b is the blockage factor defined by Hirsch and Warzee as the tangential area reduction due to the thickness of the blade.

$$b = 1 - \frac{t}{s} \quad (\text{II.A.25})$$

where t is blade thickness and s is blade spacing.

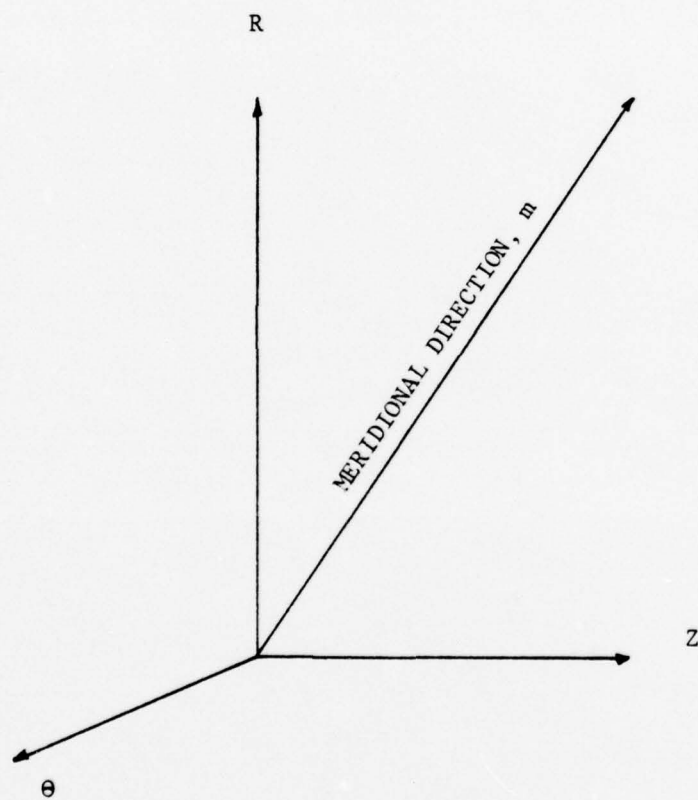


Figure 3 - MERIDIONAL PLANE

One further step in the formulation of the radial equilibrium equation for solution by the finite element method involves introducing the stream function. In cylindrical coordinates, the stream functions are defined as follows,

$$V_z = \frac{1}{\rho R b} \frac{\partial \psi}{\partial R} \quad (\text{II.A.26})$$

$$V_r = - \frac{1}{\rho R b} \frac{\partial \psi}{\partial z} \quad (\text{II.A.27})$$

Substituting these expressions into equation (II.A.16), the equation becomes,

$$\begin{aligned} \frac{\partial}{\partial R} \left(\frac{1}{\rho R b} \frac{\partial \psi}{\partial R} \right) + \frac{\partial}{\partial z} \left(\frac{1}{\rho R b} \frac{\partial \psi}{\partial z} \right) = \frac{1}{V_z} \left(\frac{\partial H}{\partial R} - T \frac{\partial s}{\partial R} \right. \\ \left. - \frac{V_\theta}{R} \frac{\partial}{\partial R} (R V_\theta) - F_{br} - F_{dr} \right] \end{aligned} \quad (\text{II.A.28})$$

The right hand side of equation (II.A.28) is applicable to the absolute flows in the stator and duct regions. For relative flows such as those in the rotor, the right hand side is modified by replacing the total enthalpy, H , by the relative total enthalpy, H_r , and the quantity V_θ/R is replaced by W_θ/R .

As a last assumption in the formulation of the governing relation for the meridional through flow radial equilibrium equation, both the radial component of the body force, F_b , and the radial component of the dissipative force, F_d , are neglected. This assumption, [Ref.1,8] does not hamper the accuracy of the results for conditions at design speed. Even though published compressor performance data used for

the test case in this thesis was obtained at 0.5 design speed, these force terms were also neglected in the computer program. As will be shown later, this assumption could possibly have had adverse effects on the predicted axial velocity profiles at the rotor hub and tip regions.

The final representation of the meridional radial equilibrium equation to be solved by the finite element method is as follows,

$$\frac{d}{dR} \left(k \frac{d\psi}{dR} \right) + \frac{d}{dz} \left(K \frac{d\psi}{dz} \right) + f = 0 \quad (\text{II.A.29})$$

where,

$$k = \frac{1}{\rho R b} \quad (\text{II.A.30})$$

and

$$f = \frac{1}{V_z} \left[T \frac{ds}{dR} - \frac{dH}{dR} + \frac{V_\theta}{R} \frac{1}{dR} (R V_\theta) \right] \quad (\text{II.A.31})$$

B. THE FINITE ELEMENT METHOD APPLIED TO THE RADIAL EQUILIBRIUM EQUATION

In order to formulate equations (II.A.29) through (II.A.31) in matrix form for solution by the finite element method, one must apply a weighted residual technique to the equations for numerical solution. The weighted residual method used here is the Galerkin's Method. The following discussion is taken from Ref. 7 with only slight changes in notation.

Rewriting equation (II.A.29) and dividing through by R, one has,

(II.B.1)

$$\frac{1}{R} \left\{ \frac{\partial}{\partial R} \left(K \frac{\partial \psi}{\partial R} \right) + \frac{\partial}{\partial z} \left(K \frac{\partial \psi}{\partial z} \right) + f \right\} = 0$$

where this equation represents the flow in the volume, V.

The boundary condition for this partial differential equation, after dividing through by R, is,

$$\frac{1}{R} \left\{ K \frac{\partial \psi}{\partial n} + \alpha_1 (\psi - \psi_0) \right\} = 0 \quad (\text{II.B.2})$$

where this equation solves the flow on the closed boundary of the volume, or, S.

By applying the weighted residual process to equations (II.B.1) and (II.B.2) and using an arbitrary weighting function, $W(r, z)$, one has

$$\int_V W(r, z) r_{vol} dV + \int_S W(r, z) r_{sur} dS = 0 \quad (\text{II.B.3})$$

where r_{vol} and r_{sur} are the volume and surface residuals respectively, or,

$$r_{vol} = - \frac{1}{R} \left\{ \frac{\partial}{\partial R} \left(K \frac{\partial \psi}{\partial R} \right) + \frac{\partial}{\partial z} \left(K \frac{\partial \psi}{\partial z} \right) + f \right\} = 0 \quad (\text{II.B.4})$$

$$r_{sur} = \frac{1}{R} \left\{ K \frac{\partial \psi}{\partial n} + \alpha_1 (\psi - \psi_0) \right\} \quad (\text{II.B.5})$$

If the solution to equation (II.B.1) was exact, both r_{vol} and r_{sur} would be equal to zero.

In order to clarify the boundary condition, equation (II.B.2), one may analyze the equation as follows.

On the surface, S , where ψ is specified,

$$\psi = \psi_0 \quad (\text{II.B.6})$$

and,

$$\alpha_1 \rightarrow \infty \quad (\text{II.B.7})$$

Similarly, on the surface, where $\frac{d\psi}{dn} = 0$, S_2 , where

$$\alpha_1 = 0 \quad (\text{II.B.8})$$

$$S_1 \cap S_2 = O, \quad S_1 \cup S_2 = S \quad (\text{II.B.9})$$

Due to the axi symmetric assumption, the final equation will not involve dV and dS but the intersection of dV and dS with the meridional plane. Therefore, one must transform the volume integral, dV , to a surface integral and the surface integral, dS , to a line integral.

Hence, let,

$d\Omega$ = intersection of dV and meridional plane

dC = intersection of dS and meridional plane

and,

$$dV = 2\pi R d\Omega$$

$$dS = 2\pi R dC$$

With this transformation, one may rewrite equation

(II.B.3) as follows,

$$\int_{\Omega} -W(R,z) \left[\frac{\partial}{\partial R} \left(K \frac{\partial \psi}{\partial R} \right) + \frac{\partial}{\partial z} \left(K \frac{\partial \psi}{\partial z} \right) + f \right] 2\pi d\Omega + \int_C W(R,z) K \frac{\partial \psi}{\partial n} 2\pi dC = 0 \quad (\text{II.B.10})$$

where on the contour, $q, \psi = \psi_0$.

One must now integrate the first term in equation (II.B.10) by parts to obtain the following,

$$\begin{aligned} & - \int_{\Omega} W \left[\frac{\partial}{\partial R} \left(K \frac{\partial \psi}{\partial R} \right) + \frac{\partial}{\partial z} \left(K \frac{\partial \psi}{\partial z} \right) \right] 2\pi d\Omega - \int_{\Omega} W \cdot f d\Omega \\ & + \int_{\Omega} K \left[\frac{\partial \psi}{\partial R} \frac{\partial W}{\partial R} + \frac{\partial \psi}{\partial z} \frac{\partial W}{\partial z} \right] d\Omega + \int_C W K \frac{\partial \psi}{\partial n} 2\pi dC = 0 \end{aligned} \quad (\text{II.B.11})$$

Inspecting the first term in equation (II.B.11), one may use the following integral theorem to simplify further

$$\int_{\Omega} \partial_{\beta} \phi d\Omega = \int_C \phi n_{\beta} dC \quad (\text{II.B.12})$$

Rewriting equation (II.B.11) gives,

$$\begin{aligned} & - \int_C W K \left[\frac{\partial \psi}{\partial R} n_R + \frac{\partial \psi}{\partial z} n_z \right] dC - \int_{\Omega} W f d\Omega + \int_{\Omega} K \left[\frac{\partial \psi}{\partial R} \frac{\partial W}{\partial R} + \frac{\partial \psi}{\partial z} \frac{\partial W}{\partial z} \right] d\Omega \\ & + \int_C W K \frac{\partial \psi}{\partial n} 2\pi dC = 0 \end{aligned} \quad (\text{II.B.13})$$

Finally, since

$$\frac{\partial \psi}{\partial n} = \frac{\partial \psi}{\partial R} n_R + \frac{\partial \psi}{\partial z} n_z \quad (\text{II.B.14})$$

equation (II.B.13) reduces to the following,

$$\int_{\Omega} \left[K \left(\frac{\partial \Psi}{\partial R} \frac{\partial W}{\partial R} + \frac{\partial \Psi}{\partial z} \frac{\partial W}{\partial z} \right) - f W \right] d\Omega = 0 \quad (\text{II.B.15})$$

One now has the final equation in the form for use by the weighted residual method using any arbitrary weighting function, $W(r,z)$. As noted previously, the Galerkin's Method will be used here which implies that the weighting functions are the same functions used in approximating the stream function, Ψ .

Before applying the finite element method, one must discretize the continuum and then approximate the unknown function, Ψ , by a set of polynomials. For this particular problem, eight-noded iso-parametric elements were chosen for discretization, see Fig 4, and the following approximating functions were used.

$$\Psi = \sum_{i=1}^8 N_i(\xi, \eta) \Psi_i \quad (\text{II.B.16})$$

where,

$N_i(\xi, \eta)$ = shape functions

Ψ_i = value of Ψ at the node

Ψ = value of Ψ at any arbitrary location within the element. The shape functions, N_i , used here are defined by the following relations as shown in Ref.10,

$$N_i(\xi, \eta) = \frac{1}{4}(1 + \xi\xi_i)(1 + \eta\eta_i)(\xi\xi_i + \eta\eta_i - 1)$$

$$N_i(\xi, \eta) = \frac{1}{2}(1 - \xi^2)(1 + \eta\eta_i) \quad (\text{II.B.17})$$

$$N_i(\xi, \eta) = \frac{1}{2}(1 + \xi\xi_i)(1 - \eta^2)$$

where the following coordinate transformations are used,

$$r = \sum_{i=1}^g N_i(\xi, \eta) r_i \quad (\text{II.B.18})$$

$$z = \sum_{i=1}^g N_i(\xi, \eta) z_i$$

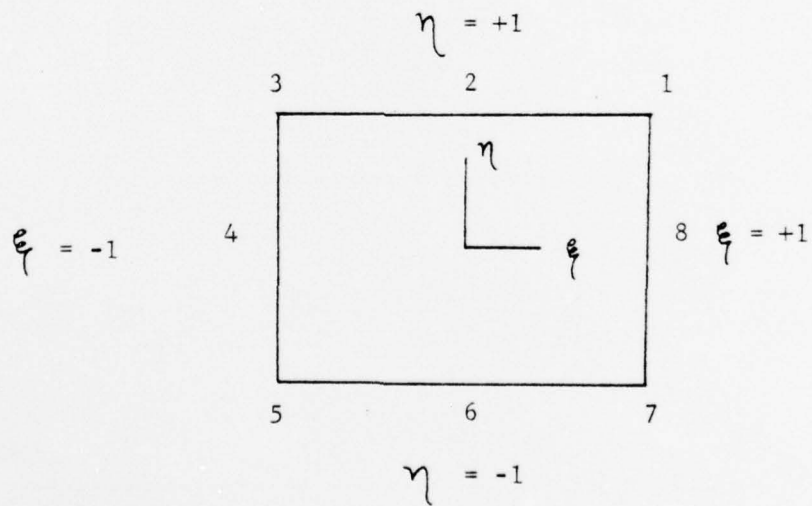
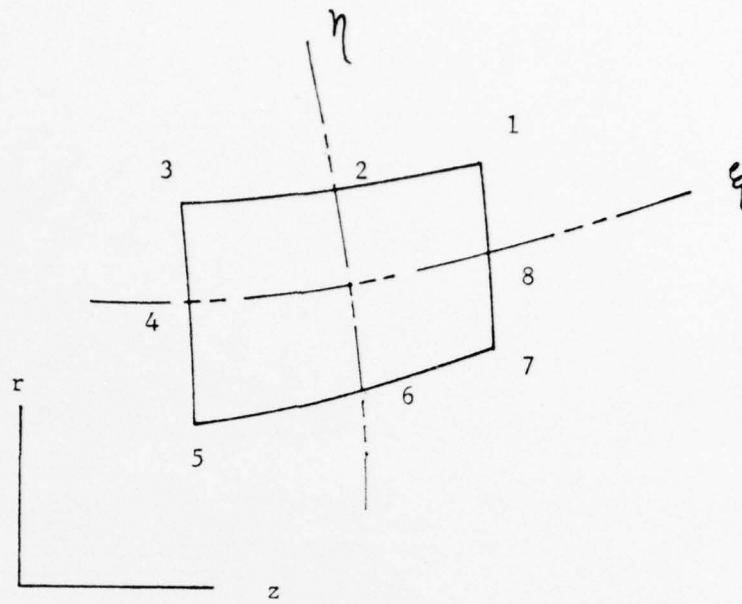


Figure 4 - ISOPARAMETRIC QUADRILATERAL ELEMENT

At this point, one is ready to apply the Galerkin Method to equation (II.B.15) by substituting equation (II.B.16) for the unknown function Ψ , and N_i for the weight function, W , which yields,

$$\int_{\Omega} k \left\{ \frac{\partial N_i}{\partial r} \sum_{j=1}^8 \Psi_j \left(\frac{\partial N_j}{\partial r} \right) + \frac{\partial N_i}{\partial z} \sum_{j=1}^8 \Psi_j \left(\frac{\partial N_j}{\partial z} \right) \right\} d\Omega - \int_{\Omega} f_i N_i d\Omega = 0 \quad (\text{II.B.19})$$

This integration yields the following system of equations which is solved for the unknown nodal Ψ ,

$$\begin{bmatrix} K_{11} & K_{12} & \cdots & K_{1n} \\ \vdots & & & \\ K_{n1} & \cdots & K_{nn} \end{bmatrix} \begin{Bmatrix} \Psi_1 \\ \vdots \\ \Psi_n \end{Bmatrix} = \begin{Bmatrix} f_1 \\ \vdots \\ f_n \end{Bmatrix} \quad (\text{II.B.20})$$

where,

$$K_{ij} = \int_{\Omega} k \left\{ \frac{\partial N_i}{\partial r} \frac{\partial N_j}{\partial r} + \frac{\partial N_i}{\partial z} \frac{\partial N_j}{\partial z} \right\} d\Omega \quad (\text{II.B.21})$$

and,

$$f_i = \int_{\Omega} f \cdot N_i d\Omega \quad (\text{II.B.22})$$

In addition since both the 'stiffness matrix', K , and the right hand side vector, $[F]$, are functions of Ψ , the system as defined by equations (II.B.20) through (II.B.21) must be solved iteratively.

At this point one has the total finite element formulation of the radial equilibrium equation as defined by equations (II.B.19) and (II.B.20). The problems which remain to be clarified are basically two fold. Firstly one

must evaluate the integrals in equations (II.B.19) and (II.B.2) by numerical methods, and secondly, the solution procedure for the non-linearity must be formulated. In Part C, both of these final steps are presented.

C. NUMERICAL INTEGRATION OF STIFFNESS MATRIX AND SOLUTION PROCEDURE

1. Numerical integration of the stiffness matrix

As noted in Section II.B, evaluation of equation (II.B.21) must be performed numerically. In addition, one realizes that the derivative expressions enclosed within the interval must be evaluated by a coordinate transformation. This is done in the following way,

Since,

$$r = \sum_{i=1}^8 N_i(\xi, \eta) r_i \quad (\text{II.C.1})$$

$$z = \sum_{i=1}^8 N_i(\xi, \eta) z_i$$

then,

$$\frac{\partial N_i}{\partial \xi} = \frac{\partial N_i}{\partial z} \frac{\partial z}{\partial \xi} + \frac{\partial N_i}{\partial r} \frac{\partial r}{\partial \xi} \quad (\text{II.C.2})$$

$$\frac{\partial N_i}{\partial \eta} = \frac{\partial N_i}{\partial z} \frac{\partial z}{\partial \eta} + \frac{\partial N_i}{\partial r} \frac{\partial r}{\partial \eta}$$

and in matrix form,

$$\begin{pmatrix} \frac{\partial N_i}{\partial \xi} \\ \frac{\partial N_i}{\partial \eta} \end{pmatrix} = \begin{bmatrix} \frac{\partial z}{\partial \xi} & \frac{\partial r}{\partial \xi} \\ \frac{\partial z}{\partial \eta} & \frac{\partial r}{\partial \eta} \end{bmatrix} \begin{pmatrix} \frac{\partial N_i}{\partial z} \\ \frac{\partial N_i}{\partial r} \end{pmatrix} \quad (\text{II.C.3})$$

Furthermore, defining the Jacobian matrix as,

$$J = \begin{bmatrix} \frac{\partial z}{\partial \xi} & \frac{\partial r}{\partial \xi} \\ \frac{\partial z}{\partial \eta} & \frac{\partial r}{\partial \eta} \end{bmatrix} \quad (\text{II.C.4})$$

then by dividing both sides of equation (II.C.3) by J , one has the following transformation,

$$\begin{pmatrix} \frac{\partial N_i}{\partial z} \\ \frac{\partial N_i}{\partial r} \end{pmatrix} = [J]^{-1} \begin{pmatrix} \frac{\partial N_i}{\partial \xi} \\ \frac{\partial N_i}{\partial \eta} \end{pmatrix} \quad (\text{II.C.5})$$

In addition, it has been shown [Ref.9] that

$$dzdr = |J| d\xi d\eta \quad (\text{II.C.6})$$

Now, with equations (II.C.5) and (II.C.6), equation (II.B.21) becomes the following,

$$K_{ij} = \int_{-1}^1 \int_{-1}^1 K \left[\frac{\partial N_i}{\partial \xi} \frac{\partial N_j}{\partial \eta} \right] \{ [J]^{-1} \}^T [J]^{-1} \left\{ \frac{\partial N_i}{\partial \xi} \frac{\partial N_j}{\partial \eta} \right\} \det [J] d\xi d\eta \quad (\text{II.C.7})$$

Equation (II.C.7) is best integrated using the Gauss-Legendre integration method since it is of the following form,

$$K_{ij} = \int_{-1}^1 \int_{-1}^1 G(\xi, \eta) d\xi d\eta \quad (\text{II.C.8})$$

or finally, [Ref.10],

$$K_{ij} = \sum_{i=1}^2 \{ A_i B_i f(\xi_i, \eta_i) \} \quad (\text{II.C.9})$$

where A_i and B_i are coefficients (Fig 5) for both two and three point Gaussian Quadrature.

At this point, one has the tools to calculate all the elements of the stiffness matrix. In like manner, the right hand side vector, f , is calculated by numerical integration.

NUMBER OF GAUSSIAN POINTS	$\pm \eta$ $\pm \xi$	$\pm A_i$ $\pm B_i$
2	0.57735 02691	1.00000 00000
3	0.77459 66692 0.00000 00000	0.55555 55555 0.88888 88888

Figure 5 - GAUSSIAN INTEGRATION POINTS

2. Solution procedure

The following is a synopsis of the basic solution process. Specific details concerning equations and methods of computer coding are covered in the proceeding section. The proceeding is meant to give the reader a preview of the solution process.

a. Discretization

Initially the machine under analysis is discretized into eight-node iso-parametric elements. The axial calculation stations are placed arbitrarily in the duct regions and along blade edges and centers for the rotor and stator as shown in Fig 6. At this point the system topology and nodal coordinates are specified.

b. Initialization

To begin the iteration process, one must assume an initial internal stream function, velocity, and density distribution. In the program, the initial internal stream function was assumed to be that of the outer boundary throughout while the velocity and density distribution was assumed to be that of the inlet.

CAVITIO NASA INSK 1

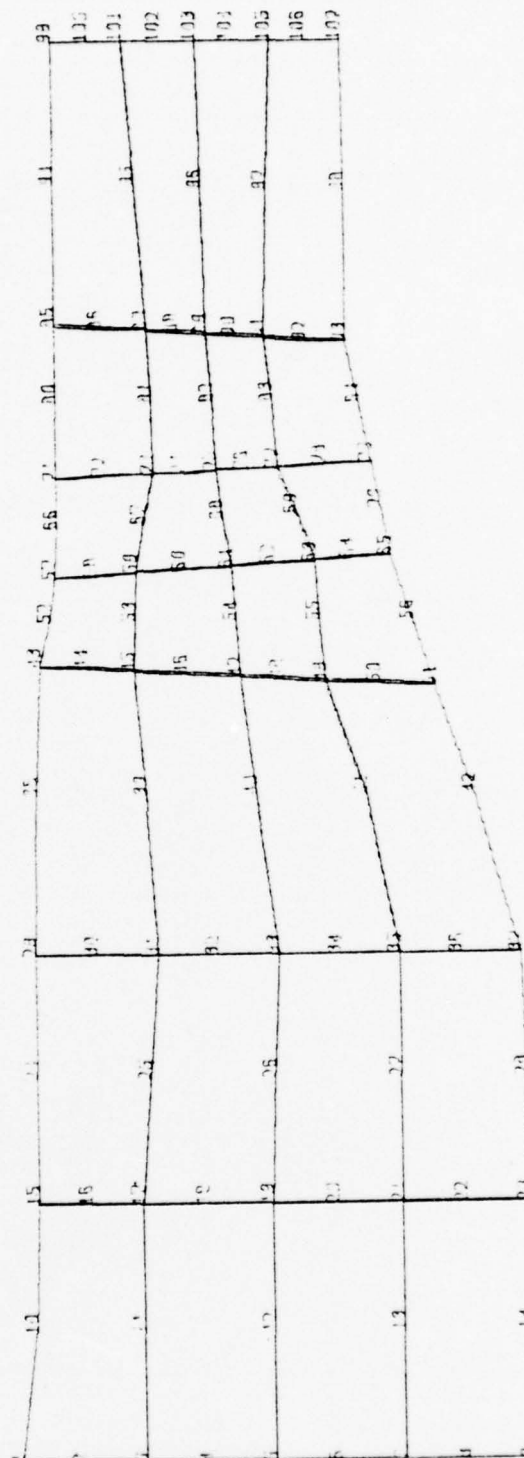


Figure 6 - COMPRESSOR DISCRETIZATION

c. Calculation of thermodynamic variables

Before calculating the right-hand side vector, f , one must obtain distributions of angular momentum, enthalpy, and entropy. This is done by first calculating the thermodynamic variables at the inlet axial station from the given inlet conditions. In order to proceed axially through the machine to calculate the nodal angular momentum, enthalpy, and entropy, the following three equations derived in Section III are used.

$$H = C_p T = \text{constant along a stator streamline}$$

$$H_R = C_p T_{tr} - \frac{(\omega r)^2}{2} = \text{constant along a rotor streamline}$$

$$r V_\theta = \text{constant along a duct streamline}$$

An example of this calculation procedure for the duct region is shown graphically in Fig 7.

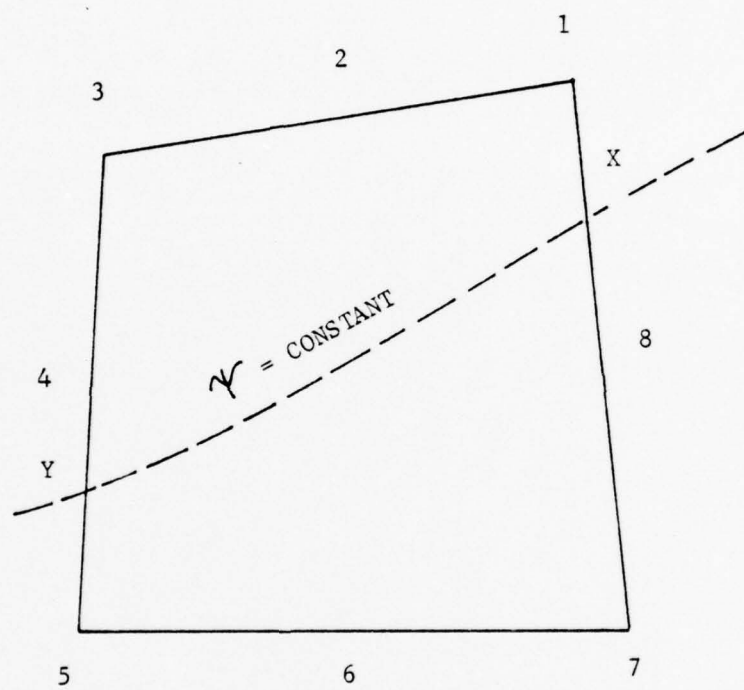


Figure 7 - DUCT ELEMENT

In this figure, the angular momentum at point X is equal to the angular momentum at point Y. More formally,

$$(rV_\theta)_X = \sum_{i=3}^5 N_i(\xi, \eta) (rV_\theta)_i = (rV_\theta)_Y \quad (\text{II.C.2.1})$$

Since the previous axial station's thermodynamic variables are known, one must now find the values of ξ and η at point Y. This is done iteratively in the following way. Since

$$\psi|_Y = \psi|_X = \sum_{i=3}^5 N_i(\xi, \eta) \psi_i \quad (\text{II.C.2.2})$$

and along the left side of the element,

$$\xi = -1 \quad (\text{II.C.2.3})$$

then equation (II.C.2.2) may be solved for η by a suitable iteration method. As will be shown in the next section, a half-interval method was used to obtain the unknown η . Once η is known, then equation (II.C.2.1) is solved for the angular momentum at point X. The rotor and stator are handled in a similar fashion. In addition, the rotor and stator deviate the flow creating a three-dimensional flow field between the blades in the respective blade row. Low speed cascade correlation data [Ref.13] was used to calculate the effective turning angles in the rotor and stator. These effects are calculated beforehand with known mass flow rate and uniform axial velocity assumptions at the rotor inlet. The results of these calculations are part of the input data routine in the form of relative and absolute flow angles at the rotor nodes and absolute flow angles at

the stator nodes. This will be shown more exactly in the next section.

d. Calculate matrices

At this point, the right hand side vector, f , and the stiffness matrix, K , are calculated.

e. Solve system of equations

The system of equations as shown in equation (II.B.20) is solved for the nodal stream function.

f. Perform relaxation iteration

Due to the strong non-linear properties of the system of equations, the following iterative scheme is necessary.

$$\psi_i^{n+1} = \psi_i^n + \alpha [\hat{\psi}_i^{n+1} - \psi_i^n] \quad (\text{II.C.2.4})$$

where α is the under relaxation factor. As will be shown in Section III, this scheme is performed only in certain regions of the machine and in addition after a specified number of iterations.

g. Update velocity and density profiles

Using the current nodal distribution of the stream function, axial and radial nodal velocity components are calculated along with a new nodal density distribution.

Again, this calculation procedure will be shown in the next section.

h. Test for convergence of ψ

Stream function convergence criteria is now tested and will determine if further iterations are necessary. The solution is said to converge if the following equation holds for all nodes.

$$\left| \frac{\psi_i^n - \psi_i^{n+1}}{\psi_i^{n+1}} \right| < \epsilon \quad (\text{II.C.2.5})$$

where ϵ is a designated requirement for convergence.

i. Summary

In summary, the eight steps involved in the solution are noted below;

- (1) Discretize the continuum.
- (2) Assume an initial stream function, velocity, and density solution.
- (3) Calculate the nodal thermodynamic variables from the given inlet conditions.
- (4) Form the right hand side vector, $f(r,z)$, and the stiffness matrix, K .
- (5) Solve the system of equations, given by, $[K] = [F]$ for a new stream function distribution.

(6) Perform relaxation iteration if required.

(7) Calculate new nodal velocity and density distributions from the current stream function solution.

(8) Test the solution for convergence, and if required, repeat steps (3) through (8) using the current nodal stream function values.

This concludes the solution description and now one is ready to more completely understand the computer program which assembles the preceding eight steps.

III. THE PROGRAM

A. OVERALL FLOWCHART AND DESCRIPTION

The overall flowchart of the program is depicted in Fig 8. Those blocks denoted by the letter 'S' are subroutines, while the remaining calculations are an integral part of the main program.

After proper dimensioning of all arrays and subsequent initialization, the input data are read and then printed. This not only presents a physical picture of the problem but also serves as a cross check to the user for correct data insertion. In addition, a subroutine is available to obtain a computer drawn plot of the mesh (Fig 6) and is a further check on proper data input.

At this point all the necessary variables have been stored and the iteration counter for stream function convergence is set. With the current nodal values of ψ and the given inlet thermodynamic conditions, the thermodynamic variables throughout the machine are calculated. From the calculated values of enthalpy and angular momentum, (isentropic flow is assumed), the right-hand side vector is calculated followed by the stiffness matrix calculation (equation II.B.21).

The system of equations (equation (II.B.20)) is now solved for the new nodal stream function distribution. It is here where for all iterations but the first that a

relaxation factor is applied as noted previously in equation (II.C.2.4). The reasoning behind not applying the relaxation scheme to the value of nodal ψ after the first iteration is the fact that the first iteration produced a close approximation to the correct stream function distribution. With this close approximation to the stream function came a velocity and density distribution which in turn was near the correct solution. It was found that if the first iteration was relaxed, the second iteration became unstable since in fact the velocities and densities were themselves farther from the true values than were assumed initially.

After testing the nodal stream function for convergence by use of equation (II.C.2.5), the calculation process is either repeated or ceased by virtue of convergence or limiting the number of iterations.

As stated previously, low speed cascade correlation data [Ref.13] were used to calculate turning angles in the blade regions. These angles were assumed constant throughout the solution and not refined after subsequent iterations. Further work on the computer program could entail an additional computational routine which would calculate the new turning angles after each iteration. A sample calculation of rotor turning angles is shown in Appendix D.

In the following sections the program structure is examined in more detail.

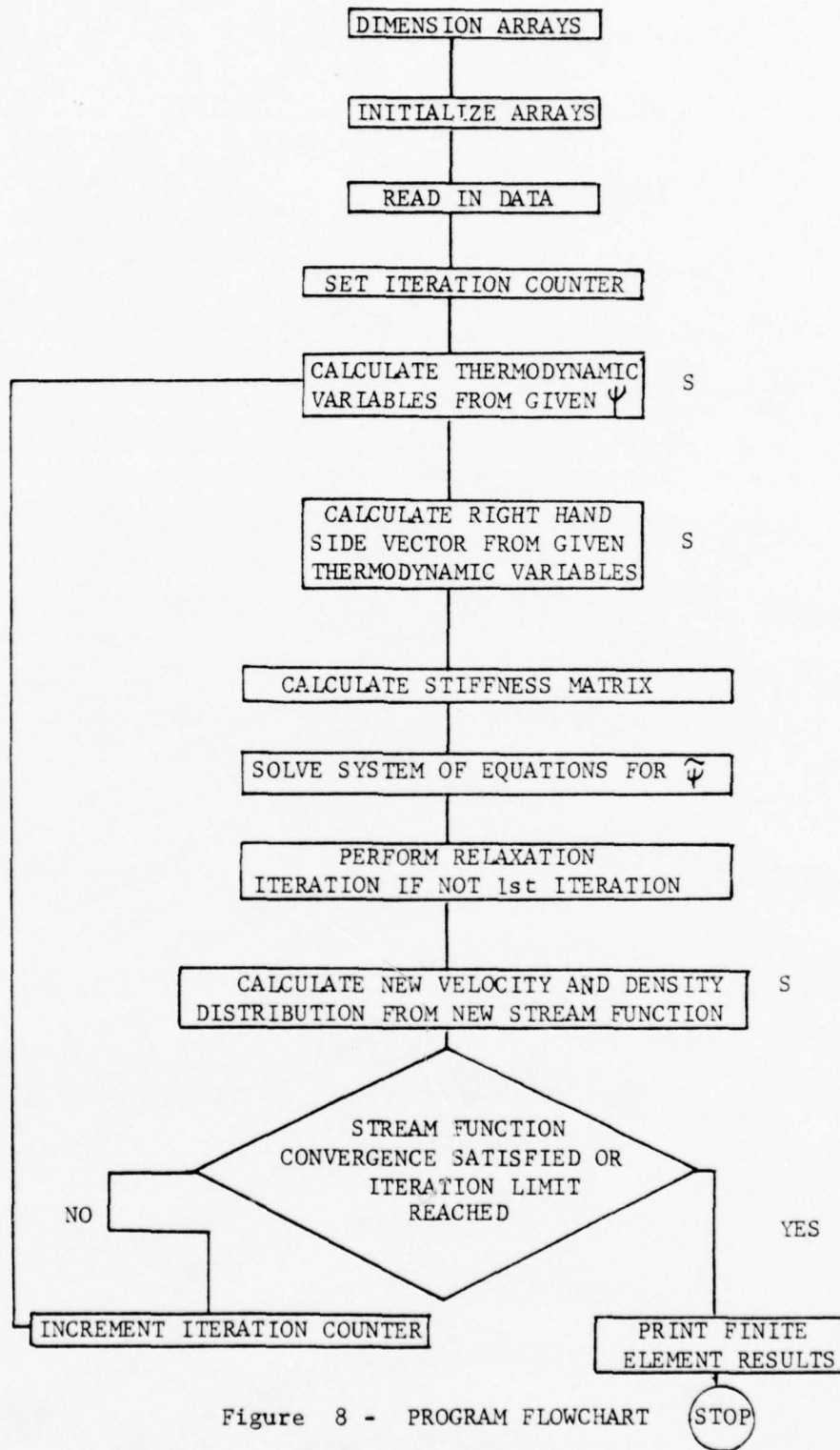


Figure 8 - PROGRAM FLOWCHART

B. THE MAIN PROGRAM

1. The input routine

The following is a description of the input data required by the program. The data are arranged into twelve categories described in the following manner.

a. category 1

Problem identification.

b. category 2

Number of nodes and number of elements.

c. category 3

Node numbers, nodal coordinates and nodal blockage factor.

d. category 4

System topology.

e. category 5

Element type; duct, rotor, or stator.

f. category 6

Absolute flow angles for rotor and stator nodes.

g. category 7

Relative flow angles for rotor nodes.

h. category 8

Inlet thermodynamic quantities.

i. category 9

Physical constants for fluid under observation.

j. category 10

First estimate of internal stream function.

k. category 11

Node numbers and specified nodal stream function.

l. category 12

Node numbers where the right hand side, $f(r,z)$, is to be calculated.

Before describing in detail the format to be followed for data insertion, it is important to note the following assumptions.

(1) Uniform flow conditions at inlet and outlet.

(2) Uniform flow conditions at rotor inlet for calculation of appropriate turning angles. This assumption is necessary to calculate the values of rotor and stator flow angles.

With this in mind , the discussion will continue.

The following describes each category in more detail.

Category 1:

Format: (20A4)

Number of cards: 1

Procedure: Enter the title of the problem in columns 1-20.

Category 2:

Format: (2I10)

Number of cards: Equal to the number of nodes in the system.

Procedure: Enter the number of nodes in columns 1-10, and the number of elements in 11-20. Both integers must be right justified.

Category 3:

Format: (I10,3F10.0)

Number of cards: Equal to the number of nodes in the system.

Procedure: Each card contains the node number followed by the Z coordinate, R coordinate, and nodal blockage factor. The coordinates are in dimensions of inches.

Category 4:

Format: (9I5)

Number of cards: Equal to the number of elements in the system.

Procedure: Each card contains nine integers right justified in columns 5, 10, 15, etc., through 45. The first integer is the element number followed by the eight nodes associated with that element. It is important to note that the nodes are read in starting with the upper right hand node and proceeding in a counterclockwise fashion around the element.

Category 5:

Format: (2I10)

Number of cards: Equal to the number of

elements.

Procedure: Enter the element number in columns 1-10, followed by the integer '1' (duct), '2' (rotor), or '3' (stator) describing the element as either in a duct, rotor, or stator region.

Category 6:

Format: (6X,A4,I10,F10.0)

Number of cards: Equal to the number of rotor and stator nodes plus one 'STOP' card.

Procedure: Enter the node number (right justified) in columns 11-20 followed by the value of the associated absolute flow angle in radians in columns 21-30. The last card in this category is a 'STOP' card entered in columns 7-10.

Category 7:

Format: (6X,A4,I10,F10.0)

Number of cards: Equal to the number of rotor nodes plus one 'STOP' card.

Procedure: Enter the node number (right justified) in columns 11-20 followed by the value of the associated relative flow angle in radians in columns 21-30. The last card in this category is a 'STOP' card.

Category 8:

Format: (7F10.0),(F10.0)

Number of cards: 2

Procedure: Enter the following quantities in the prescribed order and with the noted dimensions.

First card

Mass flow rate: (lbm/sec)

Inlet axial velocity: (ft/sec)

Outlet axial velocity: (ft/sec)

Inlet total density: (lbm/ft³)

Inlet static density: (lbm/ft³)

Inlet total pressure: (lbf/in²)

Inlet total temperature: (°R)

Second card

Speed: (RPM)

Category 9:

Format: (3F10.0)

Number of cards: 1

Procedure: Enter the following quantities in the prescribed order.

Gas constant: (ft-lbf/lbm-°R)

Ratio of specific heats

Constant pressure specific heat:
(BTU/lbm-°R)

Category 10:

Format: (F10.0)

Number of cards: 1

Procedure: Enter the first estimate of the internal stream function to be used in the first iteration.

Category 11:

Format: (6X,A4,I10,F10.0)

Number of cards: Equal to the number of nodes having a specified value of the stream function plus a 'STOP' card.

Procedure: This set of cards allows the stream function boundary conditions to be read in. A typical card contains an integer, right justified in columns 11-20 , which is the node number, followed by the value of the specified stream function in columns 21-30. The last card is a 'STOP' card.

Category 12:

Format: (6X,A4,I10)

Number of cards: Equal to the number of nodes where the right hand side is to be specified.

Procedure: Enter the node number, right justified in columns 11-20, where the right hand side is to be calculated. Again, the last card in this category is a 'STOP' card.

After all the data has been read by the program, the input data is printed and the mesh is plotted for verification by the user. The sample format is shown in Appendix C.

This concludes the input routine. The next section describes the calculation of the stiffness matrix, K.

2. Stiffness matrix evaluation

As shown previously in Section II.C.1, the following equation describes each term in the eight by eight elemental matrix.

$$K_{ij} = \int_{-1}^1 \int_{-1}^1 k \left[\frac{\partial N_i}{\partial \xi} \frac{\partial N_j}{\partial \eta} \right] \{ [J]^{-1} \}^T \{ \} \det [J] d\xi d\eta \quad (\text{III.B.2.1})$$

In addition, 'k' is defined in the following way in order to numerically integrate the equation.

$$k = \frac{1}{\sum_{i=1}^8 p_i N_i(\xi, \eta) \cdot \sum_{i=1}^8 r_i N_i(\xi, \eta) \cdot \bar{b}} \quad (\text{III.B.2.2})$$

where b is defined as the elemental blockage factor taken as an average over the eight nodes of the particular element and (ξ, η) are the defined Gauss-quadrature integration points.

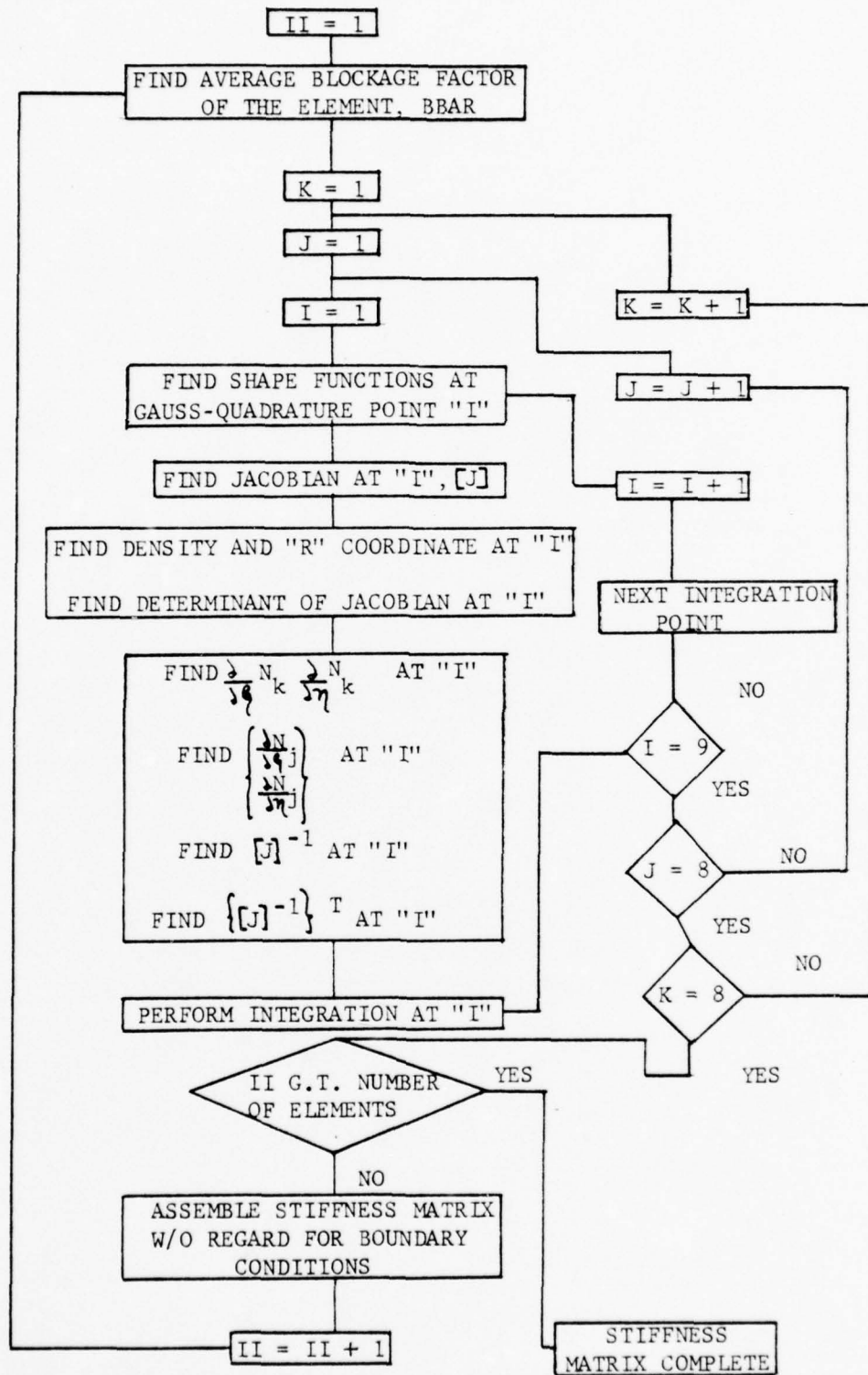


Figure 9 - STIFFNESS MATRIX EVALUATION

Fig 9 depicts the flowchart for both elemental stiffness matrix evaluation and the assemblage into the system stiffness matrix. More specifically, the figure shows a three-point Gaussian Quadrature scheme but can be changed to a two-point scheme by simply integrating four times instead of nine as shown.

The actual coding of the stiffness matrix evaluation and assemblage may be found in lines STR03510 through STR04770 in the computer program.

3. Solution of systems of equations

At this point, the system of equations are modified for the boundary conditions and solved for the nodal stream function values. An equation solving routine, DSIMQ, available in the system library was used for this purpose. It was found that no comparable savings was realised by using a banded equation solver.

4. Iteration schemes

As noted previously in Section II.C, a relaxation scheme is necessary for convergence to a solution.

Two distinct differences with regard to the iteration method were noted from that of Ref.7. Firstly, it was found that relaxation was necessary only in the rotor and stator elements and also in the duct region between the rotor outlet and stator inlet. Secondly, due to the extreme non linearity in the rotor-stator areas, a switch was required which changed the sign of α in equation (II.C.2.4) as required for stability of convergence. Clarification of

this change follows: It was found that during the initial three or four iterations, the stream function values of the rotor-stator nodes sometimes exceeded the value of the upper boundary. Due to an absence of sources within the domain of solution, this occurrence was incompatible with the boundary conditions. At this point, it was necessary to make α negative in equation (II.C.2.4). During subsequent iterations, as the solution converged, the rotor-stator regions became stable and the sign of α was returned to its positive value. This iteration proved to stabilize the solution with respect to stream function values and velocities.

The iteration procedure is coded in the computer program from lines STR05070 through STR05200.

5. The output routine

Once convergence is obtained or the number of iterations have reached the limit imposed by the user, the results are displayed. A sample output is shown in the Appendix. In addition, the units of all dependent variables are the same as those noted in the input routine.

C. THE SUBROUTINES

The following describes each of the six subroutines in the computer program. Each subsection contains a list of calling arguments and for subroutines PCAL, SLINE, and VEL, a basic flowchart. In addition, for those subroutines whose mathematical theory was not presented in Section III, a brief treatment is also given.

1. Subroutine shape

This subroutine calculates the shape functions (equation (II.B.17)) at the values of ξ and η as requested in the argument list below.

SUBROUTINE SHAPE (E,Z,SF)

E = value of ξ (input)

Z = value of η (input)

SF = eight by one vector of the eight shape functions.

2. Subroutine iacob

JACOB calculates the Jacobian matrix as defined in equation (II.C.1.4) for the value of ξ, η denoted in the argument list.

SUBROUTINE JACOB (E1,Z1,D,E,RC\$,ZC\$,RJAC)

E1 = value of η (input)

Z1 = value of ξ (input)

D = eight by one vector of $\frac{\partial N_i}{\partial \xi}$ (calculated)

E = eight by one vector of $\frac{\partial N_i}{\partial \eta}$ (calculated)

RC\$ = eight by one vector of the 'r' coordinates of the nodes associated with the element (input)

ZC\$ = eight by one vector of the 'z' coordinates of the nodes associated with the element (input)

RJAC = two by two Jacobian matrix (output)

In addition, the subroutine assumes that the vectors RC\$ and ZC\$ contain element coordinates arranged in a counter clockwise fashion beginning with the upper right corner node.

3. Subroutine sline

This subroutine calculates the thermodynamic variables throughout the machine given the inlet conditions as described in Section II.C.2. The calling arguments are defined below.

```
SUBROUTINE SLINE(UINLET,RC,PSI,WRL,H,UVEL,VVEL,TVEL,  
NODE,NNODEI,CP,TT,KK,ALP,WG,TWEL,BE,HS)
```

UINLET = Inlet axial velocity

RC = Nodal 'r' coordinates vector

PSI = Nodal stream function vector

WRL = Nodal angular momentum vector

H = Nodal total enthalpy vector

UVEL = Nodal axial velocity vector

VVEL = Nodal radial velocity vector

TVEL = Nodal absolute tangential velocity vector

NODE = Matrix containing nodes associated with the
element

INLET = Vector containing node numbers at inlet station

NNODEI = Number of nodes at inlet station

CP = Specific heat

TT = Total temperature at inlet

KK = Iteration counter
NTE = Element type vector
ALP = Nodal absolute flow angle vector
TWEL = Nodal relative tangential velocity vector
BE = Nodal relative flow angle vector
HS = Nodal static enthalpy vector

As shown in Fig 10, the basic calculation procedure begins with calculating the required energy and momentum values at the inlet station. At this point, beginning with element one, the element type is interrogated to distinguish between duct, rotor, and stator elements. If the element is in a duct region, then the streamline intersections for local nodes 2,6,7,8 and 1 (Fig 7) are determined along with the associated values of energy and angular momentum. For the rotor and stator elements, one must initially find the energy and momentum values at local nodes 3,4,5 (Fig 7) due to the discontinuities imposed by the blade edges. Once these calculations are performed, then the process for the remaining nodes in the element proceeds in a similar fashion to the duct elements.

After all the elements have been cycled through, the new distributions of nodal angular momentum and energy are returned to the main program for further computations. Specifically, these values will be used by the next subroutine, FCAL, for calculation of the right hand side vector.

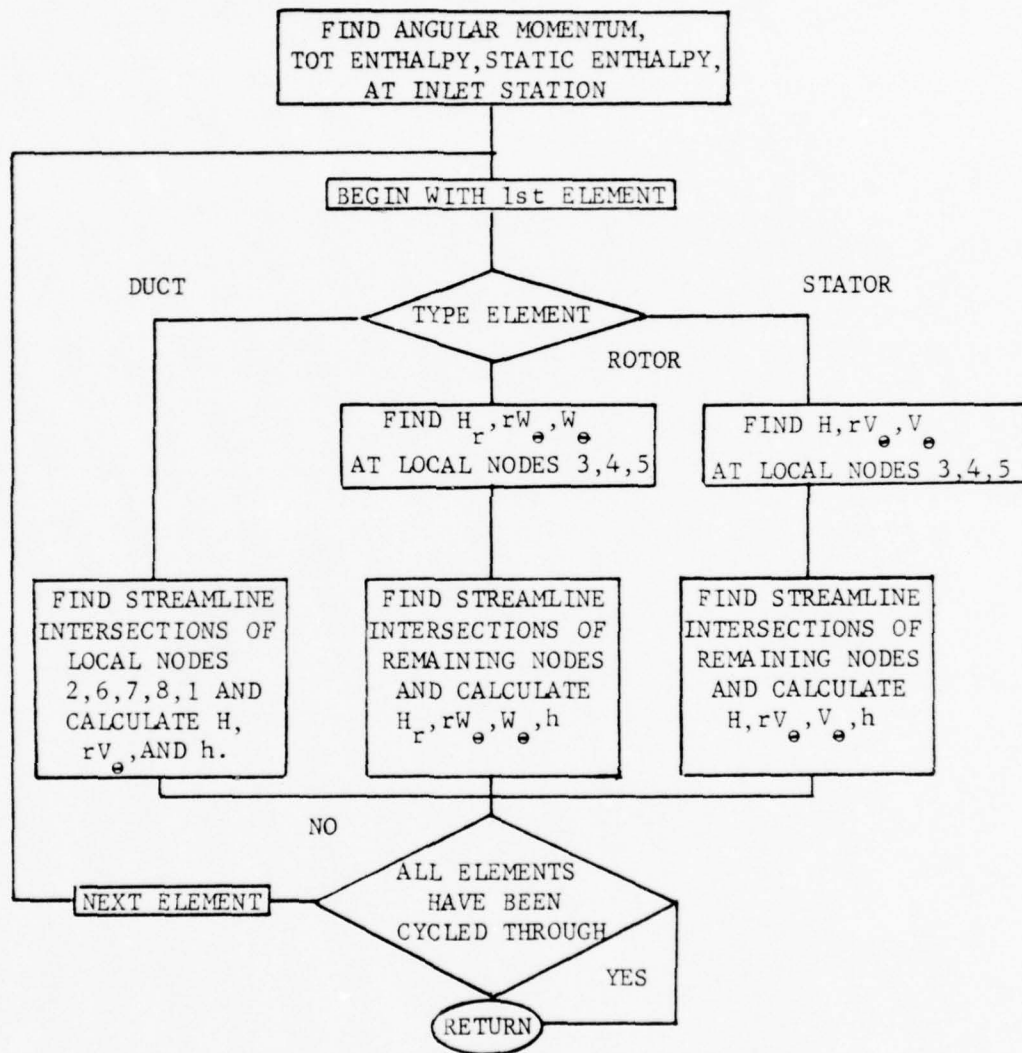


Figure 10 - SUBROUTINE SLINE

4. Subroutine fcal

FCAL calculates the right hand side vector as defined by equations (II.A.31) and (II.B.21). Using the identical coordinate transformations for numerical integration as described in Section II.C, the final equation to be coded is the following,

$$f_i = \int_{-1}^1 \int_{-1}^1 \frac{N_i}{\sum N_i V_{2i}} \cdot \frac{\sum N_i V_{0i}}{\sum N_i R_i} \left\{ (LJ^{-1}(2,1) \cdot \frac{\partial N_i}{\partial \xi} + J(2,2) \cdot \frac{\partial N_i}{\partial \eta}) (W_i - H_i) \right\} \det J d\xi d\eta \quad (\text{III.C.4.1})$$

where isentropic flow is assumed, and,

W_i = angular momentum

(III.C.4.2)

H_i = total enthalpy

The argument list is defined below. In addition, only those variables in the list which have not been defined previously are described.

SUBROUTINE FCAL(F,W,H,ZA,EA,UVEL,RC,ZC,WRL,TVEL,NFS,
NODE,NN,NE,NNFSP,TWEL,NPE)

F = Right hand side vector, $f(r,z)$

W = vector of gaussian quadrature coefficients

ZA = Vector of ξ ; gaussian quadrature points

EA = Vector of η ; gaussian quadrature points

NFS = Vector containing nodes where the right hand side

is to be specified

NN = number of nodes

NE = number of elements

NNFSP = Number of nodes where the right hand side is specified

Fig 11 depicts the basic flowchart for the subroutine. To initialize the procedure, one begins with the first node (upper right hand corner) of the first element. A switch is then applied which determines if the right hand side is to be calculated at the node or if a stream function value has been specified. This information is transferred from the main program through the argument list. Once the node is allowed through the switch, then the integration process is started at the first integration point. As in Section III.A.2, the flowchart depicts a three-point Gauss Quadrature scheme. After the integration has been completed, a switch determines if all the local nodes in the element have been cycled through and if so, then the assembly of the elemental vector, F_e , is performed to build the system right hand side vector, F . Finally, the subroutine determines if all the elements have been examined in order to signal completion of the right hand side vector. At this point, the vector, $F(r,z)$, is returned to the main program for problem solution.

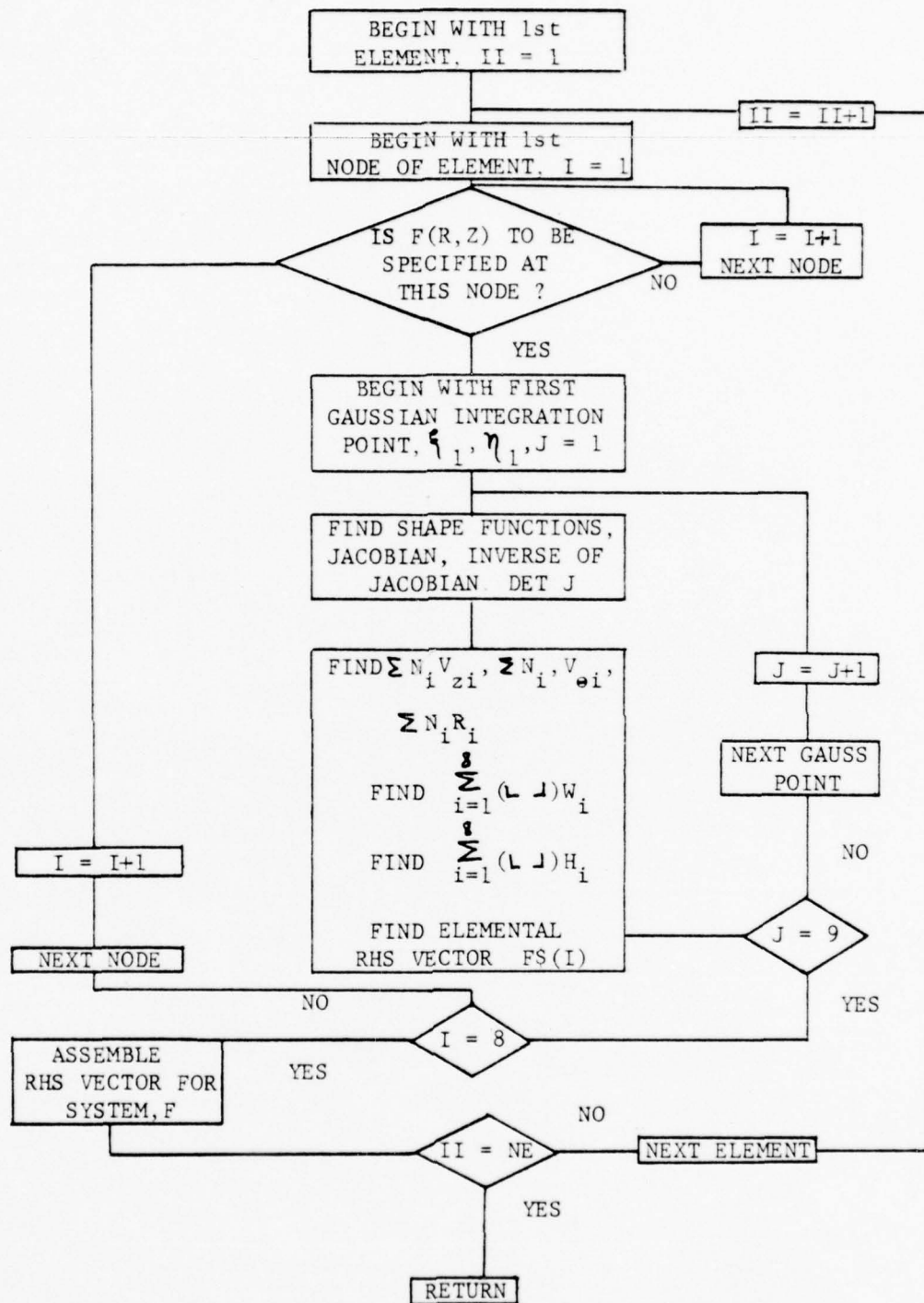


Figure 11 - SUBROUTINE FCAL

5. Subroutine vel

This subroutine calculates axial and radial velocities and also densities at each of the nodes from a known stream function distribution. As noted previously in Section II.C.2, both velocity and density profiles are updated after obtaining the latest value of nodal stream function.

The velocity calculation proceeds from the stream function equations,

$$V_z = \frac{1}{prb} \frac{\partial \psi}{\partial r} \quad (\text{III.C.5.1})$$

$$V_r = - \frac{1}{prb} \frac{\partial \psi}{\partial z} \quad (\text{III.C.5.2})$$

where 'b' is the tangential blockage factor. Since r , p , and ψ are of the following form,

$$\begin{aligned} r &= \sum_{i=1}^8 r_i N_i \\ p &= \sum_{i=1}^8 p_i N_i \\ \psi &= \sum_{i=1}^8 N_i \psi_i \end{aligned} \quad (\text{III.C.5.3})$$

then the equation for the axial velocity, V_z , becomes,

$$V_z = \frac{1}{b \sum_{i=1}^8 p_i N_i \sum_{i=1}^8 N_i r_i} \left[\sum_{i=1}^8 \frac{\partial N_i}{\partial r} \psi_i \right] \quad (\text{III.C.5.4})$$

Again, since the shape function, $N_i(\eta, \gamma)$, is not an

implicit function of 'r' and 'z', one must use equation (II.C.1.5) to obtain the proper derivatives for computation of equation (III.C.5.4). For example, from equation (III.C.5),

$$\sum_{i=1}^8 \frac{\partial N_i}{\partial r} = \sum_{i=1}^8 \left[J^{-1}(1,1) \cdot \frac{\partial N_i}{\partial \xi} + J^{-1}(1,2) \frac{\partial N_i}{\partial \eta} \right] \quad (\text{III.C.5.5})$$

At this point, with equation (III.C.5.5) substituted into equation (III.C.5.4), one has the complete expression for the axial velocity as functions of ξ, η . One proceeds similarly for expressing the radial velocity, V , in terms of ξ and η .

In order to calculate the nodal density, one uses the following density relation for flows in the stator and duct regions.

$$\frac{p}{p_t} = \left(1 - \frac{n-1}{2a_0} V^2 \right)^{\frac{1}{n-1}} \quad (\text{III.C.5.6})$$

where p_t is the stagnation density.

Since,

$$V^2 = (V_z^2 + V_r^2)(1 + \tan^2 \alpha) \quad (\text{III.C.5.7})$$

then,

$$\frac{p}{p_t} = \left[1 - \frac{n-1}{2a_0} \left(\frac{1}{r b} \right)^2 (\psi_r^2 + \psi_z^2) (1 + \tan^2 \alpha) \right]^{\frac{1}{n-1}} \quad (\text{III.C.5.8})$$

Since the density appears on both sides of the equation, the new nodal density is obtained iteratively at the node.

For the relative flows in the rotor, the following relation for static density is used [Ref.14].

$$\frac{p}{p_t} = \left[1 - (\gamma-1) \frac{\omega R V_\theta^2}{a_o^2} - \frac{(\gamma-1)}{2} \frac{W^2 - \omega^2 R^2}{a_o^2} \right]^{\frac{1}{\gamma-1}} \quad (\text{III.C.5.9})$$

Again, the solution of the nodal density is obtained in an iterative fashion.

In the following argument list, only those variables not defined in the previous subroutine descriptions are noted.

SUBROUTINE VEL(NE,NN,RC,NODE,G,RG,TT,RHOT,RHON,ZC,PSI,RHO,B,UIINLET,UVEL,VVEL,RHOSTA,NTE,ALP)

G = Ratio of specific heats

RG = Gas constant

RHOT = Total density at the inlet

RHON = Work vector which contains the new nodal density distribution

RHO = Nodal static density vector

B = nodal blockage factor vector

RHOSTA = Static density at the inlet station

The basic flowchart for SUBROUTINE VEL is shown in Fig 12. Beginning with the first node of the first element, the Jacobian matrix (equation (II.C.1.4)) and its inverse

are found. At this point the partial derivatives with respect to 'r' and 'z' of the shape functions are found as noted in equation (III.C.5.5). A switch then allows those nodes not at the inlet station to pass and calculates the new density and velocities at the nodes. For those nodes at the inlet, the velocities and static densities are retained at the given inlet conditions. This is done to maintain boundary condition integrity for the solution. After cycling through all elements, the subroutine returns the new nodal velocity and density distributions to the main program.

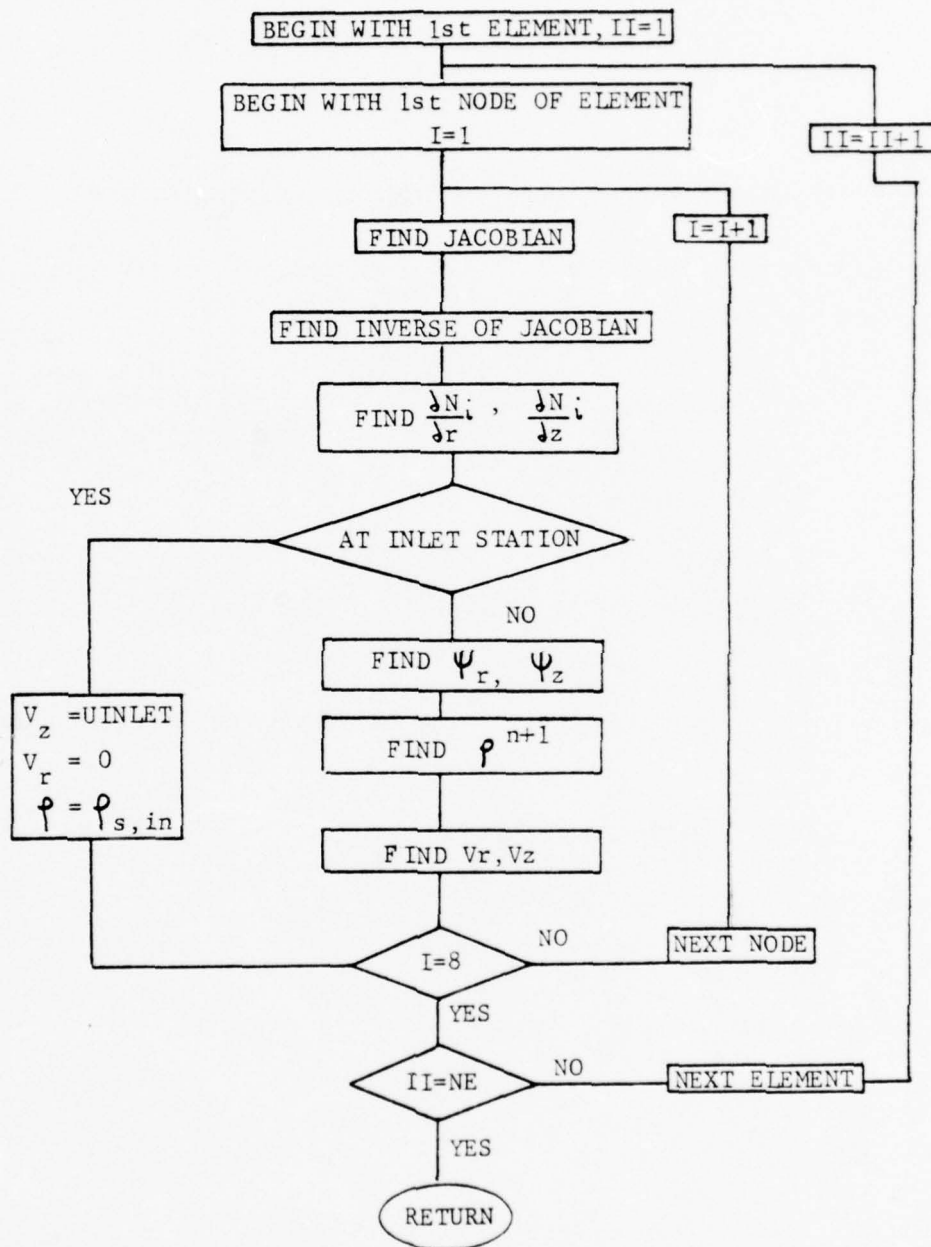


Figure 12 - SUBROUTINE VEL

6. Subroutine mplot

This subroutine utilizes the Calcomp plotter to depict the mesh topology of the machine under observation.

```
SUBROUTINE MPlot(RC,ZC,NODE,NN,NE)
```

This completes the description of the main program and associated subroutines. In the next section, a test case is carried through from data input to final results.

IV. TEST CASES AND RESULTS

The program was tested by using published performance data [Ref.12] of the NASA Task-1 stage transonic compressor. The compressor was discretized into twenty-eight elements and 107 nodes with 15 axial calculation stations (Fig 6). The speed was 0.5 design speed with a mass flow of 107.6 lbm/sec. In addition, uniform flow was assumed both at the inlet and outlet stations. Turning angles for the rotor and stator were pre calculated assuming uniform conditions at the rotor inlet and using NASA SP-36 blade correlation data [Ref.13]. These absolute and relative flow angles were assumed constant throughout the iterative procedure as they were an integral part of the input data. The Appendix contains a listing of the input data and output results for the NASA Task-1 transonic compressor with test conditions noted. To compare the accuracy of the predicted flow with actual laboratory observations, computed axial velocity profiles at the rotor inlet, rotor outlet, stator inlet, and stator outlet were compared with experimental results. In addition numerical results from Ref.7 were also compared.

Fig 13-16 show the computer predictions plotted with the experimental values and the numerical solutions obtained by Hirsch and Warzee. The profiles shown were obtained after ten iterations and using a relaxation factor of 0.2. The figures show that the best overall agreement with experimental data occurred in the stator inlet and outlet. In this region the worst error was 17% which occurred at the stator tip inlet. The average error throughout the stator region with respect to experimental data was 6.6%.

The rotor hub and tip outlet area exhibited instabilities in density convergence using equation III.C.5.9. Specifically, the density solution converged to within 8% at the rotor outlet tip and hub. It was found that by not allowing the nodal density at these nodes to go below a critical value of 0.06 lbm/cu ft, the solution for the stream function converged. By allowing the nodal densities at the rotor outlet tip and hub to go below this critical value, the computed velocities at these nodes became increasingly large and the argument within the brackets of equation III.C.5.9 became less than one. This prevented continuation of the iterations for the stream function solution. In addition, the rotor tip outlet exhibited more instability than the rotor hub outlet. The static density at the rotor hub outlet oscillated about a value of 0.062 lbm/cu ft while the rotor tip outlet was constantly driven to the critical value of 0.06 lbm/cu ft. One method attempted to alleviate this problem was the following. Since a half-interval iteration routine was used, one trial run involved reversing the direction of consecutive guesses when the density iteration did not converge. It was found however, that after three to four iterations of the system of equations, the static densities at the rotor outlet tip and hub were again driven to smaller and smaller values which led to instability once more. The nodal densities converged at all interior points of the rotor edge and mid-blade regions and also at all the rotor inlet nodes. By including all rotor nodes, the average error with respect to experimental data was 27.5%.

Fig 17 shows a plot of convergence criteria, ϵ , versus the number of iterations for a relaxation factor of 0.2. The stability of convergence is shown to initially decrease and then after the third iteration oscillates about an approximate value of 28%. It is important to note that this curve represents the maximum value of ϵ as shown in equation

(II.C.2.5). In addition, the curve in actuality represents the oscillation of nodal stream function values in the rotor/stator regions since in fact this is where the non-linearity is the greatest.

V. CONCLUSIONS AND RECOMMENDATIONS FOR FURTHER STUDY

Agreement with both experimental data and numerical solution of Ref.7 was best in the stator region to within 8%. Predicted axial velocity profiles in the rotor inlet area were within 26.2% of experimental results. The instabilities with respect to static density solutions are prevalent. One of the reasons for this numerical disagreement with Hirsch and Warzee is the isentropic assumption imposed by the present program. Recommendations for further study on the project include the addition of entropy variations in the rotor and stator blade regions. This would necessitate the use of blade correlation data [Ref.13] for loss predictions and involve additional input data plus program additions to Subroutine's SLINE and FCAL.

RADIUS (IN)

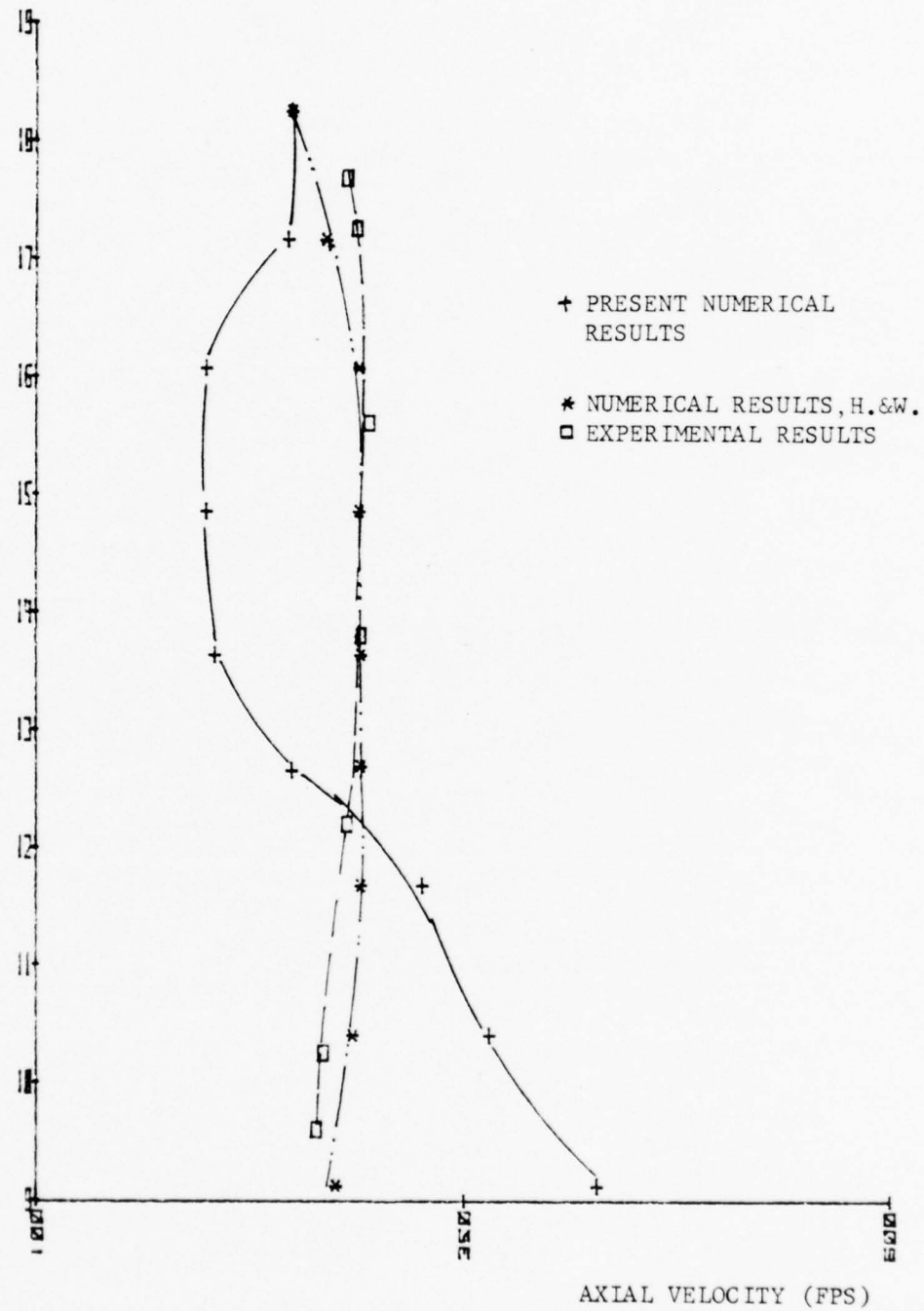


Figure 13 - AXIAL PROFILE AT ROTOR INLET

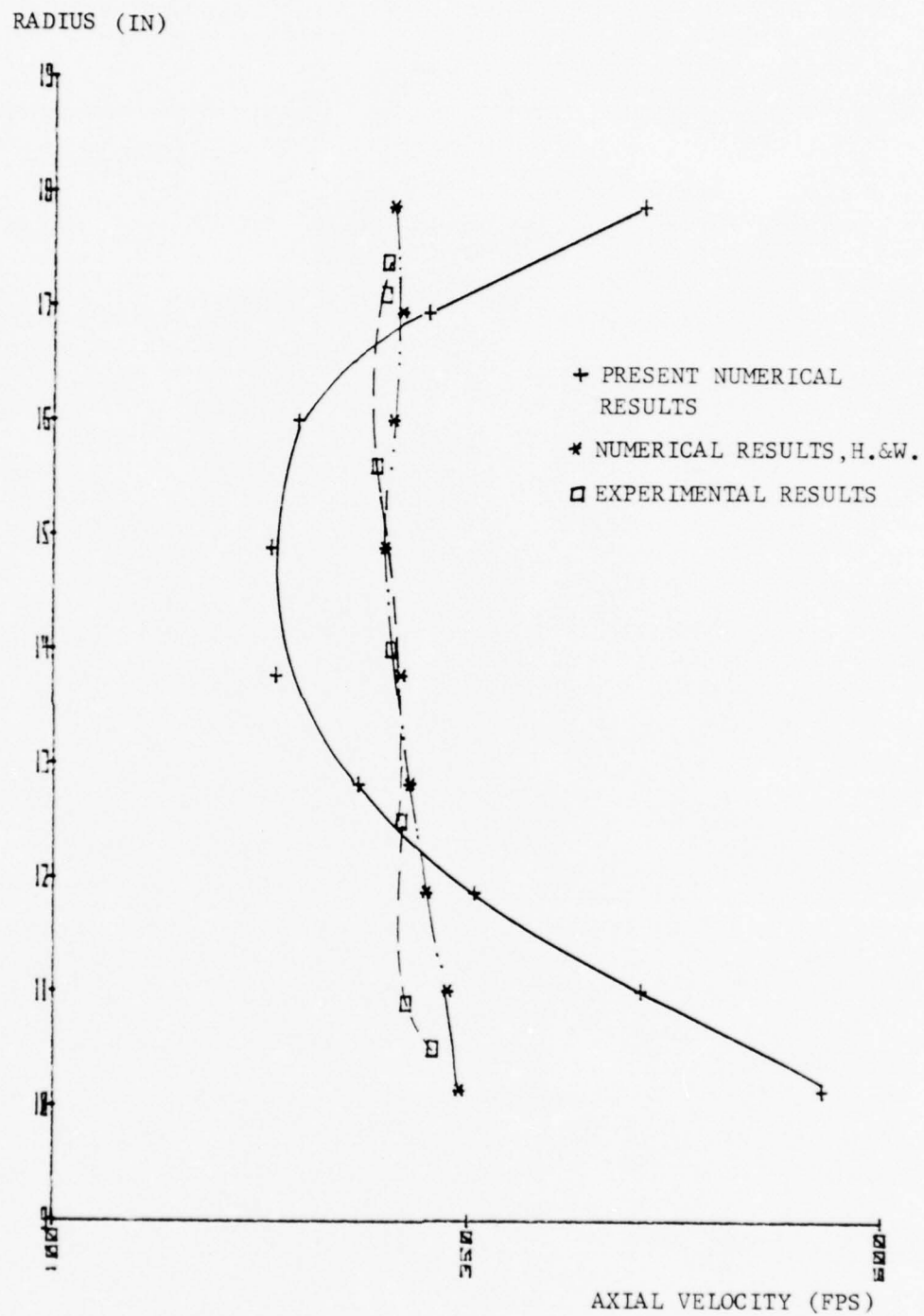


Figure 14 - AXIAL PROFILE AT ROTOR OUTLET

RADIUS (IN)

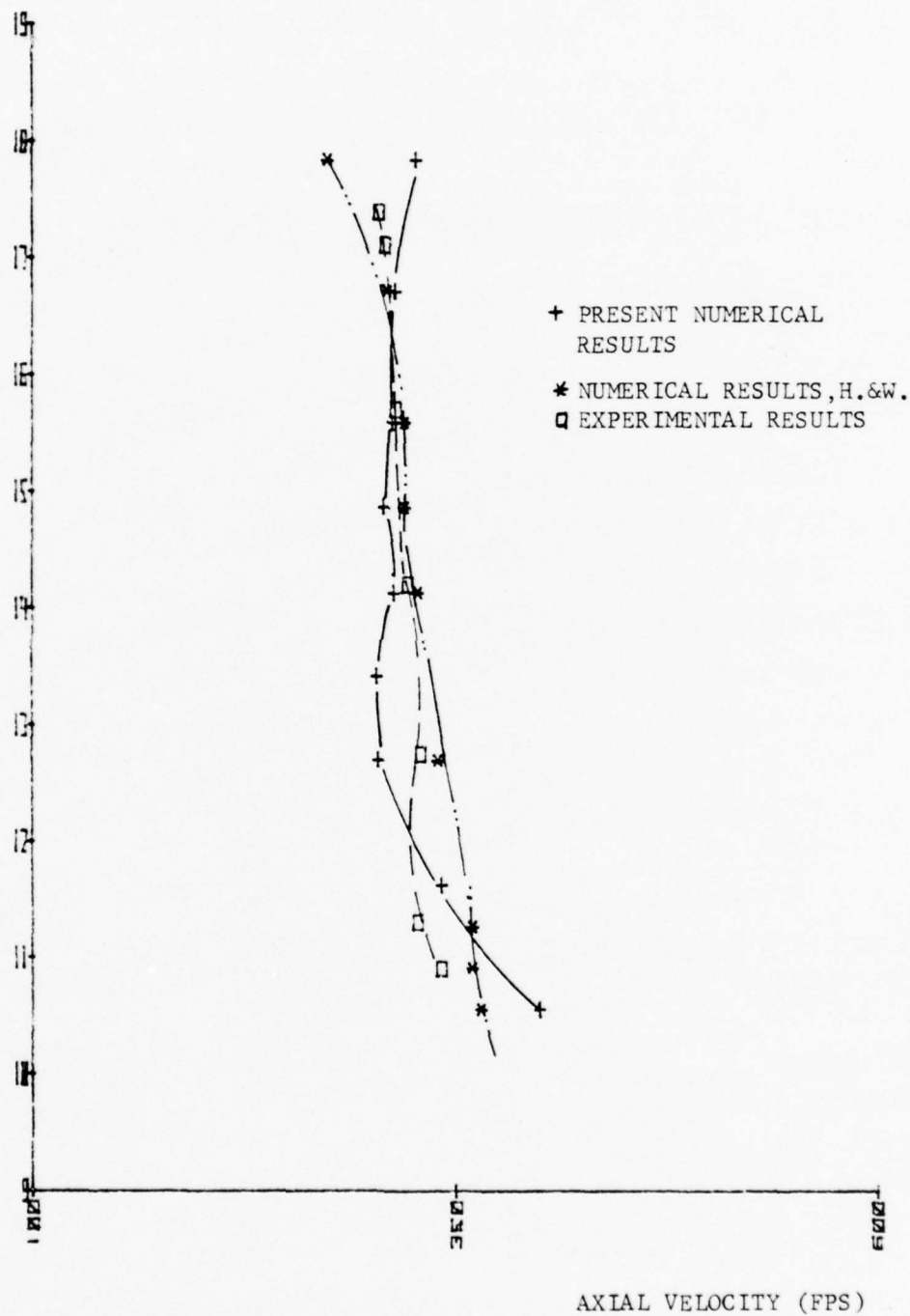


Figure 15 - AXIAL PROFILE AT STATOR INLET

RADIUS (IN)

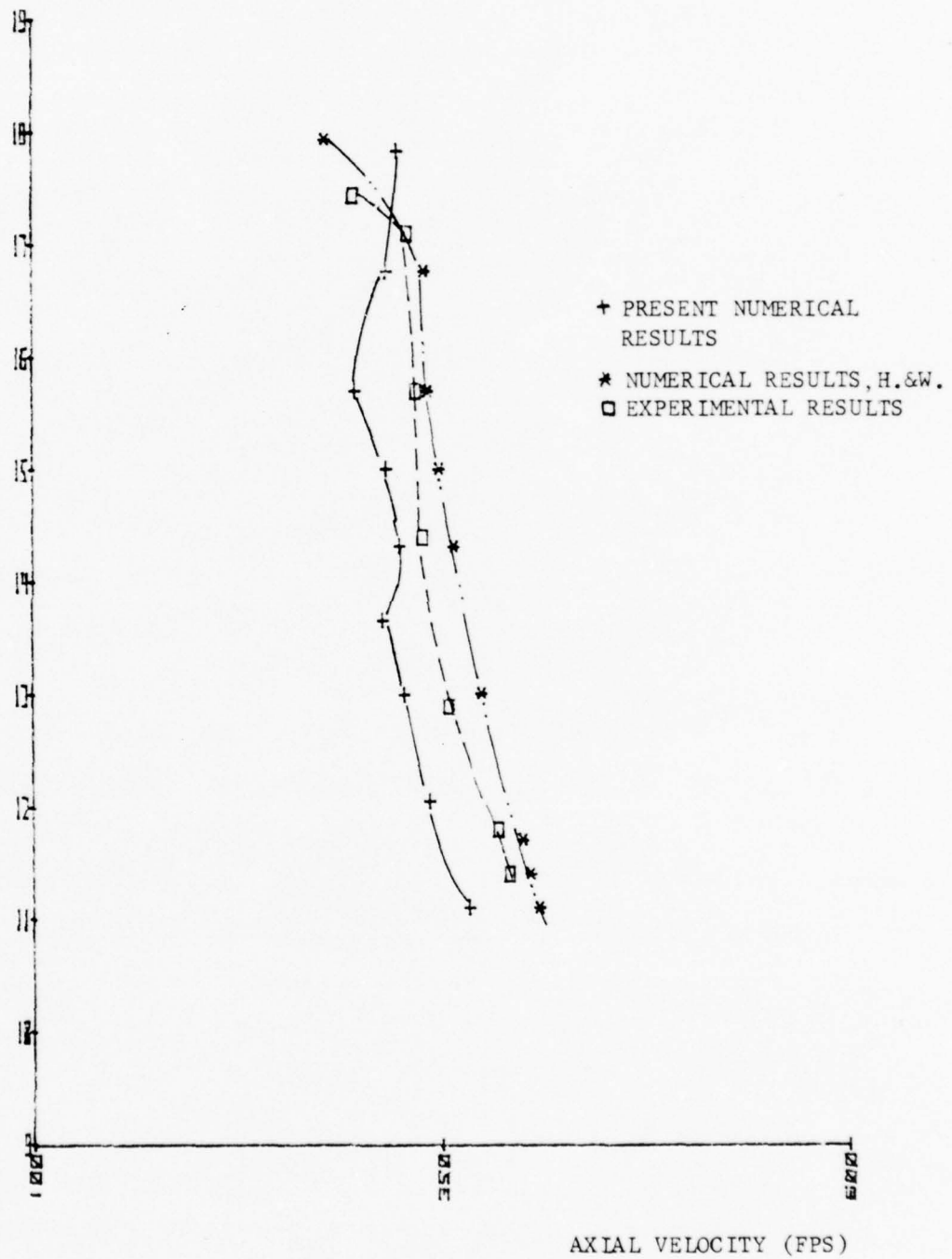


Figure 16 - AXIAL PROFILE AT STATOR OUTLET

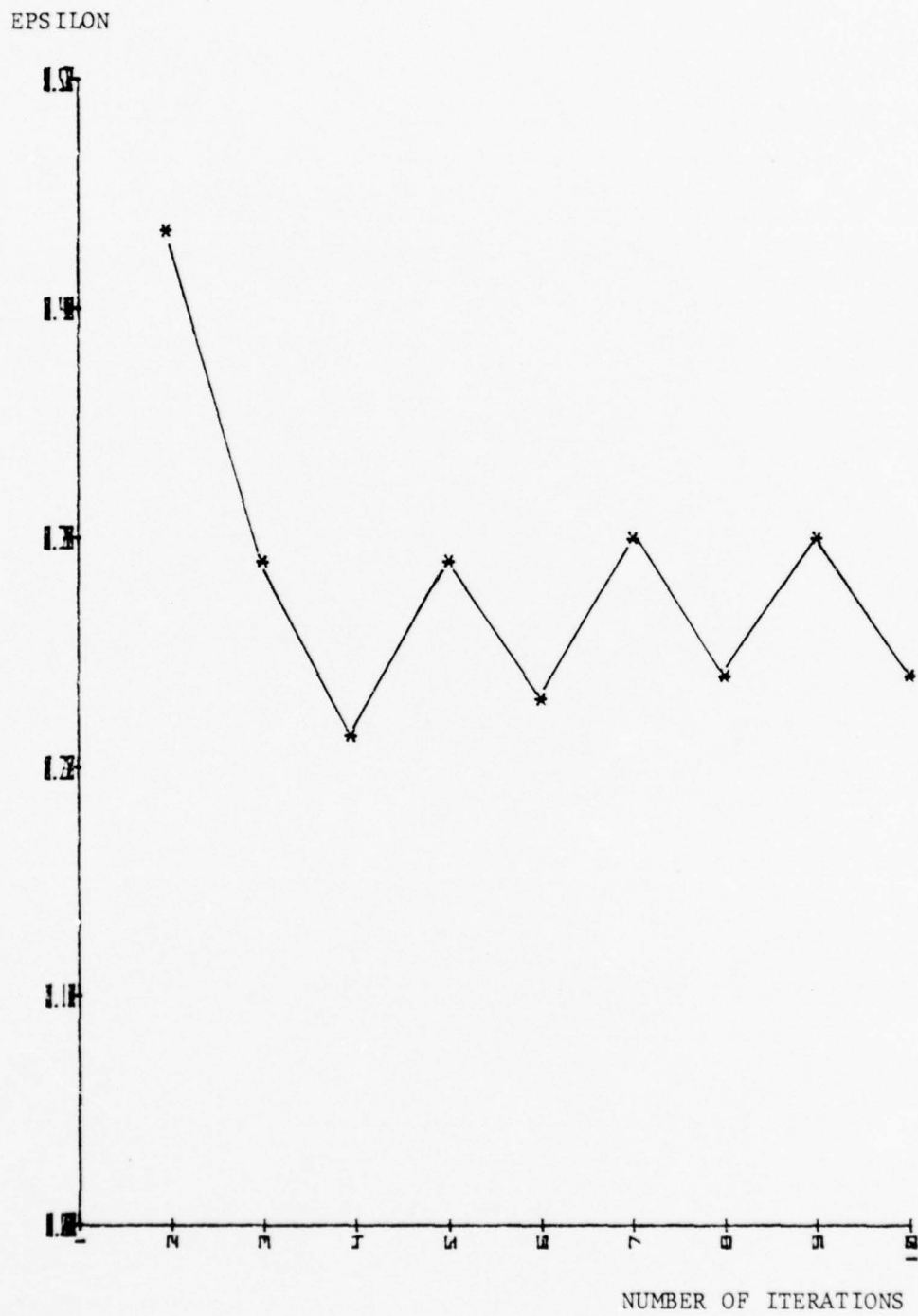


Figure 17 - EPSILON VS. ITERATIONS

APPENDIX A COMPUTER PROGRAM

```

C C C C C C C C
C C C

      THE FINITE ELEMENT METHOD APPLIED TO TWO-DIMENSIONAL.
      AXI-SYMMETRIC, INVISCID, COMPRESSIBLE FLOW IN A TURBO-
      MACHINE. STREAM FUNCTION FORMULATION IS USED ALONG WITH
      EIGHT-NODE ISOPARAMETRIC ELEMENTS. TWO POINT OR THREE
      POINT GAUSSIAN QUADRATURE FOR NUMERICAL INTEGRATIONS
      ARE USED.
      IMPLICIT REAL*8(A-H,P-Z)
      DATA NREAD/4/
      DATA NWRITE/7/
      DATA STOP/1,STOP/

      DIMENSION ALL ARRAY VARIABLES

      DIMENSION RJAC(2,2), ROW(1,2), COL(2,1), EMS(8,8), RIJAC(2,2), R(40)
      DIMENSION EM(107,107), F(107), PSI(107), RHS(107), TIJAC(2,2)
      DIMENSION PROD1(1,2), PROD2(1,2), PROD3(1,1), FNZ1(1,1), FNZ2(1,1), W(9)
      DIMENSION U(8), F(8), SF(8), ZA(9), EA(9), RHOF(40)
      DIMENSION UVEL(107), VVEL(107), PRES(107), RC$(8)
      DIMENSION ZC$(8), RC(107), RHO(107), B(107), RHON(107)
      DIMENSION WRL(107)
      DIMENSION TVFL(107), PSI0(107), H(107), ALP(107), TWEL(107), BE(107)
      DIMENSION RTEMP(107), HS(107)
      DIMENSION NPSIS(107), NFIS(107)
      DIMENSION NFS(107), NPSI(107), NODE(28,8), N(8), LI(2), MI(2), INLET(10)
      DIMENSION IULET(10), NTE(40), TITLE(10)

      TWO-POINT GAUSSIAN POINTS.

      DATA ZA/.5773502700,-.5773502700,~.5773502700,~.5773502700/
      DATA EA/.5773502700,.5773502700,-.5773502700,-.5773502700/

      THREE-POINT GAUSSIAN POINTS.

      DATA ZA/.77459666924200,.77459666924200,~.77459666924200,
      10.00,0.00,0.00,-.77459666924200,-.77459666924200,
      2~.77459666924200/
      DATA EA/.77459666924200,0.00,-.77459666924200,
      1.77459666924200,0.00,-.77459666924200,
      2.77459666924200,0.00,-.77459666924200/
      WEIGHING FUNCTIONS FOR 3 PT. GAUSSIAN QUAD. PTS.

      DATA W/.308641975200,.493827160400,.308641975200,
      1.493827160400,.790123456600,.493827160400,
      2.308641975200,.493827160400,.308641975200/

      READ(NREAD,50)TITLE
      READ IN TITLE

```



```

160      EM$(I,J) = 0.00
      CONTINUE
      DO 165 I = 1,NE
      NTE(I) = 0
      RHOE(I) = 0.00
      R(I) = 0.00
      DO 165 J = 1,8
      NODE(I,J) = 0
      CONTINUE
      READ NODE NUMBERS, NODAL COORDINATES (IN INCHES), AND NODAL BLOCKAGE FACTOR. INLET STATION ZC(I) MUST BE = 0.00. LAST NODAL ZC(NN) MUST BE AT THE OUTLET STATION.
165      DO 170 J = 1,NN
      READ(NR,1000) I, ZC(I), RC(I), B(I)
      FORMAT(110,3F10.0)
      CONTINUE
1000      READ IN SYSTEM TOPOLOGY, I.E., ELEMENT NO. AND LOCAL NODE NUMBERS. STARTING AT UPPER RIGHT HAND CORNER AND TRAVERSING IN A CCW FASHION AROUND THE QUADRILATERAL.
170      DO 180 L = 1,NE
      READ(NR,1010) J, NODE(J,1), NODE(J,2), NODE(J,3), NODE(J,4)
      1, NODE(J,5), NODE(J,6), NODE(J,7), NODE(J,8)
      FORMAT(9I5)
      CONTINUE
1010      DO 185 I = 1,NE
      READ(NR,1011) J, NTE(J)
      FORMAT(2I10)
      CONTINUE
185      READ IN TYPE OF ELEMENT: NTE(I)=1(DUCT), NTE(I)=2(ROTOR)
      NTE(I)=3(STATOR)
      DO 185 I = 1,NE
      READ(NR,1011) J, NTE(J)
      FORMAT(2I10)
      CONTINUE
1011      READ IN STATOR/ROTOR NODAL ABS FLOW ANGLES
      REMEMBER THAT THIS ASSUMES UNIFORM FLOW CONDITIONS AT ROTOR INLET.
185      DO 186 I = 1,NN
      READ(NR,1012) WORD, J, ANGLE
      FORMAT(6X,A4,I10,F10.0)
      IF(WORD.EQ.STOP) GOTO 1014
      ALP(J) = ANGLE
      CONTINUE
1012      READ IN ROTOR NODAL REL FLOW ANGLES.
186      DO 186 I = 1,NN
      READ(NR,1012) WORD, J, ANGLE
      FORMAT(6X,A4,I10,F10.0)
      IF(WORD.EQ.STOP) GOTO 1014
      ALP(J) = ANGLE
      CONTINUE
1014

```

```

STR00970
STR00980
STR00990
STR01000
STR01010
STR01020
STR01030
STR01040
STR01050
STR01060
STR01070
STR01080
STR01090
STR01100
STR01110
STR01120
STR01130
STR01140
STR01150
STR01160
STR01170
STR01180
STR01190
STR01200
STR01210
STR01220
STR01230
STR01240
STR01250
STR01260
STR01270
STR01280
STR01290
STR01300
STR01310
STR01320
STR01330
STR01340
STR01350
STR01360
STR01370
STR01380
STR01390
STR01400
STR01410
STR01420
STR01430
STR01440

```



```

C      FINDING THE NODES, PROCEED TO CALCULATE THE VALUES OF
C      PSI BY ASSUMING UNIFORM FLOW CONDITIONS AT INLET AND
C      OUTLET BY ASSUMING RHO = STATIC DENSITY AT INLET(RHOSTA)
C
231      FIND NODES AT INLET STATION
C
      KIS = 0
      DO 231 I = 1, NN
      IF(ZC(I).NE.0.00)GOTO231
      KIS = KIS + 1
      INLET(KIS) = I
      NNODEI = KIS
      CONTINUE
C
232      FIND NODES AT OUTLET STATION
C
      KIS = 0
      DO 232 I = 1, NN
      IF(ZC(I).NE.ZC(NN))GOTO232
      KIS = KIS + 1
      IULET(KIS) = I
      NNODEO = KIS
      CONTINUE
C
      READ NODES WHERE PSI IS SPECIFIED
C
      DO 190 I = 1, NN
      READ(NREAD,1020)WORD,NPSP,PS
      FORMAT(6X,A4,I10,F10.0)
      IF(WORD.EQ.STOP)GOTO191
      NPISIS(I) = NPSP
      PSI(NPISIS(I)) = PS
      CONTINUE
C
190      COUNT NODES HAVING SPECIFIED PSI
C
191      NPSPSI = 1-I
      INSERT INLET PSI DISTRIBUTION FROM 'U' VEL DISTRIBUTION.
      DO 192 I = 1, NNODEI
      NPISIS(NPSPSI + I) = INLET(I)
      PSI(INLET(I)) = UINLET*(RC(INLET(I))*2 - RC(NNODEI)**2)/2.00
      PSI(IULET(I)) = PSI(INLET(I))*RHO(INLET(I))*B(INLET(I))/144.00
      PSIO(INLET(I)) = PSI(INLET(I))
      CONTINUE
      NNPSSI = NNPSSI + NNODEI
      INSERT OUTLET PSI DISTRIBUTION FROM 'U' VEL DISTRIBUTION
      DO 193 I = 1, NNODEO
      NPISIS(NNPSSI + I) = IULET(I)
      PSI(IULET(I)) = UOULET*(RC(IULET(I))*2 - RC(NN)**2)/2.00
      PSI(IULET(I)) = PSI(IULET(I))*RHO(IULET(I))*B(IULET(I))/144.00
      PSIO(IULET(I)) = PSI(IULET(I))
      CCNTINUE
C
193

```

```

C
C
C
C
C
1030
200
201
C
C
C
210
C
C
220
C
C
C
C
C
C
221
1038
1040
1045
1050
1060
1062

```

```

RECOUNT NUMBER OF NODES WITH SPECIFIED PSI BY INCLUDING
THE INLET AND OUTLET NODES.

NNSPSI = NNPSI + NNODEO
READ NODES WHERE F(R,Z) IS SPECIFIED
DO 200 I = 1, NN
READ(NREAD,1030) WORD,NFSP
FORMAT(6X,A4,I10)
IF(WORD.EQ.'STOP')GOTO201
NFS(I) = NFSP
CONTINUE
NNFSP = I-1

NFIS IS A LIST OF THE INDICES OF THE KNOWN F(R,Z)
DO 210 I = 1,NNFSP
NFIS(I) = NFS(I)
CONTINUE

NPSI IS A LIST OF THE INDICES IF THE KNOWN PSI
DO 220 I = 1,NNSPSI
NPSI(I) = NPSIS(I)
CONTINUE

NTOTF = NNFSP
NTOTF IS THE TOTAL NUMBER OF KNOWN F(R,Z)

NTOTP = NNSPSI
NTOTP IS THE TOTAL NUMBER OF KNOWN PSI
PRINT ALL INPUT DATA

GO TO 1101
WRITE(NWRITE,1038)TITLE
FORMAT(1X,20X,10A4)
WRITE(NWRITE,1040)NN,NE
FORMAT(1X,4X,NO. OF NODES = ,I3,/,5X,
1,NO. OF ELEMENTS = ,I2)
WRITE(NWRITE,1045)
FORMAT(1X,20X,SUMMARY OF NODAL COORDINATES')
WRITE(NWRITE,1050)
FORMAT(1X,NODE,5X,Z(I),11X,R(I),11X,B(I),
1,7X,ABS FLOW ANG,3X,REL FLOW ANG)
WRITE(NWRITE,1060)(I,ZC(I),RC(I),B(I),ALP(I),BE(I),I=1,NN)
FORMAT(1X,13,2X,E13.6,2X,E13.6,2X,E13.6,2X,E13.6)
WRITE(NWRITE,1062)
FORMAT(1X,20X,SYSTEM TOPOLOGY',/,2X,'ELEMENT',
110X,NODES',40X,'TYPE OF ELEMENT')
WRITE(NWRITE,1063)(I,NODE(I,1),NODE(I,2),NODE(I,3),NODE(I,4)

```

```

STR02410
STR02420
STR02430
STR02440
STR02450
STR02460
STR02470
STR02480
STR02490
STR02500
STR02510
STR02520
STR02530
STR02540
STR02550
STR02560
STR02570
STR02580
STR02590
STR02600
STR02610
STR02620
STR02630
STR02640
STR02650
STR02660
STR02670
STR02680
STR02690
STR02700
STR02710
STR02720
STR02730
STR02740
STR02750
STR02760
STR02770
STR02780
STR02790
STR02800
STR02810
STR02820
STR02830
STR02840
STR02850
STR02860
STR02870
STR02880

```



```

DO 4321 I = 1, NN
  UVEL(I) = UVEL(I)/12.D0
  VVEL(I) = VVEL(I)/12.D0
CONTINUE
DO 2345 I = 1, NN
  UVEL(I) = UVEL(I)*12.D0
  VVEL(I) = VVEL(I)*12.D0
CONTINUE
  COMPARE 'NEW STREAM FUNCTION' DISTRIBUTION WITH 'OLD
  STREAM FUNCTION DISTRIBUTION.
  X = 0.D0
DO 430 I = 1, NN
  IF(PSI(I).EQ.0.D0)GOTO421
  EPS = DABS((PSI(I) - PSI(I))/PSI(I))
  GOTO422
EPS = DABS(PSI(I) - PSI(I))
IF (X.GT.EPS)GOTO430
X = EPS
CONTINUE

  ASK IF STREAM FUNCTION CONVERGENCE CRITERION BEEN SATISFIED?
  IF IT HAS.....WRITE RESULTS
  IF NOT.....ITERATE ONCE MORE.

  KK = KK + 1
  IF(X.LE.1.D-01)GOTO450
  WRITE (NWRITE,1400)KK,X
  FORMAT(1,' ',LARGEST EPS FOR ITERATION ',I2,' IS ',D19.12)
  IF (KK.LT.2)GOTO1500
  WRITE(NWRITE,1600)KK,X
  FORMAT(1,' ',PROGRAM TERMINATED ON ITERATION NO.',I3,'/,
  1, RESULTS WHICH FOLLOW ARE FOR CONVERGENCE EPSILON = ',D19.12)
  GOTO1104
  WRITE(NWRITE,1102)KK
  FORMAT(1,' ',ITERATION NO.',I3,' COMPLETE',/,
  1, STREAM FUNCTION CONVERGENCE NOT YET SATISFIED.,/,
  1, NEXT ITERATION IS IN PROGRESS.)
  NEXT ITERATION
  ZEROIZE STIFFNESS MATRIX AND RIGHT HAND SIDE VECTOR TO
  PREPARE FOR NEXT ITERATION.

DO 460 I = 1, NN
  F(I) = 0.D0
DO 460 J = 1, NN

```

```

STR05280
STR05290
STR05300
STR05310
STR05320
STR05330
STR05340
STR05350
STR05360
STR05370
STR05380
STR05390
STR05400
STR05410
STR05420
STR05430
STR05440
STR05450
STR05460
STR05470
STR05480
STR05490
STR05500
STR05510
STR05520
STR05530
STR05540
STR05550
STR05560
STR05570
STR05580
STR05590
STR05600
STR05610
STR05620
STR05630
STR05640
STR05650
STR05660
STR05670
STR05680
STR05690
STR05700
STR05710
STR05720
STR05730
STR05740
STR05750

```


[illegible]


```

130      CONTINUE
C
C
131      FIND F$(NODE(I1,I1))
C
C
300      XX = SUMH + (SUMV/SUMR)*SUMW
200      XX = (SF(I1)/SUMU)*XX*DETJ
C
C
C      F$(I1) = F$(I1) + XX*W(J)
CONTINUE
CONTINUE
C
C
C      ASSEMBLE RIGHT HAND SIDE VECTOR.
C
C
C      N(1) = NODE(I1,1)
C      N(2) = NODE(I1,2)
C      N(3) = NODE(I1,3)
C      N(4) = NODE(I1,4)
C      N(5) = NODE(I1,5)
C      N(6) = NODE(I1,6)
C      N(7) = NODE(I1,7)
C      N(8) = NODE(I1,8)
C      DO 400 I$ = 1,8
C      I = N(I$)
C      F(I) = F(I) + F$(I$)
C      CONTINUE
C
C
400      DO 500 I = 1,8
C      F$(I) = 0.00
C      CONTINUE
C
C
500      NEXT ELEMENT.
C
C
100      CONTINUE
RETURN
DEBUG SUBCHK
END
SUBROUTINE JACOB(E1,Z1,D,E,RC$,ZC$,RJAC)
IMPLICIT REAL*8(A-H,P-Z)
C
C
C      THIS SUBROUTINE CALCULATES THE JACOBIAN MATRIX FOR SUBSE-
C      QUENT NUMERICAL INTEGRATIONS BY GAUSSIAN QUADRATURE.
C
C      DIMENSION RJAC(2,2),D(8),E(8),RC$(8),ZC$(8)
C      RJAC(1,1) = 0.00
C      RJAC(1,2) = 0.00
C      RJAC(2,1) = 0.00
C      RJAC(2,2) = 0.00
C      D(1) = (E1 + 2.00*Z1 + 2.00*Z1*E1 + E1*E1)/4.00
C
STR07200
STR07210
STR07220
STR07230
STR07240
STR07250
STR07260
STR07270
STR07280
STR07290
STR07300
STR07310
STR07320
STR07330
STR07340
STR07350
STR07360
STR07370
STR07380
STR07390
STR07400
STR07410
STR07420
STR07430
STR07440
STR07450
STR07460
STR07470
STR07480
STR07490
STR07500
STR07510
STR07520
STR07530
STR07540
STR07550
STR07560
STR07570
STR07580
STR07590
STR07600
STR07610
STR07620
STR07630
STR07640
STR07650
STR07660
STR07670

```


STR07680
STR07690
STR07700
STR07710
STR07720
STR07730
STR07740
STR07750
STR07760
STR07770
STR07780
STR07790
STR07800
STR07810
STR07820
STR07830
STR07840
STR07850
STR07860
STR07870
STR07880
STR07890
STR07900
STR07910
STR07920
STR07930
STR07940
STR07950
STR07960
STR07970
STR07980
STR07990
STR08000
STR08010
STR08020
STR08030
STR08040
STR08050
STR08060
STR08070
STR08080
STR08090
STR08100
STR08110
STR08120
STR08130
STR08140
STR08150

```

D(2) = -(Z1 + Z1*E1)
D(3) = (-E1 + 2.00*Z1 + 2.00*Z1*E1 - E1*E1)/4.00
D(4) = (-1.00 + E1*E1)/2.00
D(5) = (E1 + 2.00*Z1 - 2.00*Z1*E1 - E1*E1)/4.00
D(6) = -Z1 + Z1*E1
D(7) = (-E1 + 2.00*Z1 - 2.00*Z1*E1 + E1*E1)/4.00
D(8) = (1.00 - E1*E1)/2.00
E(1) = (Z1 + 2.00*E1 + Z1*Z1 + 2.00*Z1*E1)/4.00
E(2) = (1.00 - Z1*Z1)/2.00
E(3) = (-Z1 + 2.00*E1 + Z1*Z1 - 2.00*Z1*E1)/4.00
E(4) = -E1 + E1*Z1
E(5) = (Z1 + 2.00*E1 - Z1*Z1 - 2.00*Z1*E1)/4.00
E(6) = (-1.00 + Z1*Z1)/2.00
E(7) = (-Z1 + 2.00*E1 - Z1*Z1 + 2.00*Z1*E1)/4.00
E(8) = -(E1 + Z1*E1)
DO 100 I = 1,8
  RJAC(1,1) = RJAC(1,1) + D(I)*ZC$(I)
  RJAC(1,2) = RJAC(1,2) + D(I)*RC$(I)
  RJAC(2,1) = RJAC(2,1) + E(I)*ZC$(I)
  RJAC(2,2) = RJAC(2,2) + E(I)*RC$(I)
CONTINUE
RETURN
DEBUG SUBCHK
END

```

100

```

SUBROUTINE VEL(NN,RC,NODE,G,RG,TT,RHOT,RHON,ZC,PSI,RHO,B,UINLET
1,UVEL,VVEL,RHOSTA,ALP,BE,H,WC)

```

CCCCCCCC

THIS SUBROUTINE CALCULATES U AND V VELOCITIES AND A NEW
NODAL DENSITY FROM A KNOWN PSI DISTRIBUTION AT EACH OF
THE NODES IN THE SYSTEM. IN ADDITION, THE CALL STATEMENT
TRANSFERS THE NUMBER OF ELEMENTS, NODAL COORDINATES, LOCAL
NODE NUMBERS, RATIO OF SPECIFIC HEATS, GAS CONSTANT, TOTAL
TEMPERATURE, TOTAL DENSITY, THE LATEST CALCULATED NODAL
STREAM FUNCTION, DENSITY DISTRIBUTION, NODAL BLOCKAGE FAC-
TOR, AND INLET VELOCITY CONDITIONS.

```

IMPLICIT REAL*8(A-H,P-Z)
DIMENSION RJAC(2,2),PSI(107),D(8),E(8),UVEL(107),VVEL(107)
DIMENSION RC$(8),ZC$(8),RC(107),ZC(107),RHO(107),E1(8),Z1(8)
DIMENSION DR(8),DZ(8),B(107),RHON(107),H(107),ALP(107),BE(107)
DIMENSION NODE(28,8),LI(2)
DIMENSION MI(2)
DATA Z1/1.00,0.00,-1.00,-1.00,0.00,1.00,1.00,0.00/
DATA E1/1.00,1.00,1.00,0.00,-1.00,-1.00,-1.00,0.00/
DO 100 I = 1,NE
  RC$(1) = RC(NODE(11,1))
  RC$(2) = RC(NODE(11,2))
  RC$(3) = RC(NODE(11,3))
  RC$(4) = RC(NODE(11,4))

```



```

301      IDEN = IDEN + 1
      IF(NODE(II,I).LT.43)GOTO300
      IF(NODE(II,I).GT.65)GOTO300
      XM = (XL + XR)/2.D0
      RI = RC(NODE(II,I))
      BI = B(NODE(II,I))
      WI = (PSIZ**2 + PSIR**2)/((XM*RI*BI)**2)
      WI = (W1*144.D0*144.D0/32.174D0)/(DCOS(BETA)**2)
      UI = (WG*RI)**2/(144.D0*32.174D0)
      AI = (G - 1.D0)*(W1 - UI)/(2.D0*G*RG*TT)
      A2 = DSQR((PSIR**2+PSIZ**2)/((XM*RI*BI)**2))*DTAN(ALPHA)
      A2 = (G - 1.D0)*(WG*RI)**2/(G*RG*TT)
      A2 = A2*12.D0/32.174D0
      RHON(NODE(II,I)) = RHOT*((1.D0-A2-A1)**(1.D0/(G-1.D0)))
      GOTO315
300      AI = (G - 1.D0)/(2.D0*G*RG*TT)
      XM = (XL + XR)/2.D0
      AI = AI/((XM
      *RC(NODE(II,I))*B(NODE(II,I))**2)
      AI = AI*144.D0*144.D0/32.174D0
      AI = 1.D0 - AI*(PSIZ**2 + PSIR**2*(1.D0 + DTAN(ALPHA)**2))
      AI = AI*(1.D0/(G - 1.D0))
      RHON(NODE(II,I)) = RHOT*AI
      EPS = RHON(NODE(II,I)) - XM
      X4 = DABS(EPS)
      IF(X4.LT.1.D-06)GOTO250
      IF(IDEN.EQ.10)GOTO250
      IF(EPS.LT.0.D0)GOTO310
      XL = XM
      GOTO301
      XR = XM
      GOTO301
250      IF(XM.GT.6.D-02)GOTO255
      XM = 0.6D-01
255      RHON(NODE(II,I)) = XM
      C
      C
      FIND UVEL AND VVEL
      UVEL(NODE(II,I)) = PSIR/(XM
      *RC(NODE(II,I))*B(NODE(II,I)))
      VVEL(NODE(II,I)) = UVEL(NODE(II,I))*144.D0*12.D0
      VVEL(NODE(II,I)) = -PSIZ/(XM
      *RC(NODE(II,I))*B(NODE(II,I)))
      VVEL(NODE(II,I)) = VVEL(NODE(II,I))*144.D0*12.D0
      GO TO 200
10      UVEL(NODE(II,I)) = UINLET
      VVEL(NODE(II,I)) = 0.D0
      RHON(NODE(II,I)) = RHOSTA
      CONTINUE
200      C
      C
      NEXT ELEMENT
100      CONTINUE

```

```

STR08640
STR08650
STR08660
STR08670
STR08680
STR08690
STR08700
STR08710
STR08720
STR08730
STR08740
STR08750
STR08760
STR08770
STR08780
STR08790
STR08800
STR08810
STR08820
STR08830
STR08840
STR08850
STR08860
STR08870
STR08880
STR08890
STR08900
STR08910
STR08920
STR08930
STR08940
STR08950
STR08960
STR08970
STR08980
STR08990
STR09000
STR09010
STR09020
STR09030
STR09040
STR09050
STR09060
STR09070
STR09080
STR09090
STR09100
STR09110

```

```

500 DO 500 I = 1, NN
C      RHO(I) = RHON(I)
C      CONTINUE

C      RETURN
C      DEBUG SUBCHK
C      END
C      SUBROUTINE SLINE(UINLET, RC, PSI, WRL, H, UVEL, VVEL, TVEL, NODE
C      1, INLET, NNODEI, NE, CP, TT, KK, NTE, ALP, WG, TWEL, BE, HS)
C      IMPLICIT REAL*8(A-H, P-Z)
C      DIMENSION PSI(107), SF(8), UVEL(107), VVEL(107), RC(107), WRL(107)
C      DIMENSION TVEL(107)
C      DIMENSION H(107), ALP(107), TWEL(107), BE(107), HS(107)
C      DIMENSION EL(8), NODE(28,8)
C      DIMENSION INLET(10), NTE(40)
C      DATA EL/1.00, 1.00, 1.00, 0.00, -1.00, -1.00, -1.00, 0.00/
C
C      THIS SUBROUTINE CALCULATES THE THERMODYNAMIC VARIABLES
C      THROUGHOUT THE SYSTEM FROM GIVEN INLET CONDITIONS AT THE
C      DUCT. THIS IS DONE BY INITIALLY SEARCHING FOR THE
C      STREAMLINES AT EACH NODE AND THEN USING THE ASSUMPTION
C      THAT IN A DUCT REGION THE SWHRL (R*VTHETA) IS CONSTANT
C      IN ROTOR, HREL IS CONSTANT; AND IN STATOR, H IS CONSTANT.
C
C      FIND WHIRL AT INLET
C      FIND V THETA AT INLET
C      INSERT TOT ENTHALPY AT INLET NODES.
C      INSERT STATIC ENTHALPY AT INLET NODES
C
C      MM = 0
C      THEVEL = UINLET*DTAN(ALP(1))
C      DO 100 I = 1, NNODEI
C      WRL(INLET(I)) = RC(INLET(I))*THEVEL
C      H(INLET(I)) = CP*TT
C      HS(INLET(I)) = CP*TT - (UINLET**2)/7.20935D06
C      CONTINUE
C
C      BEGIN WITH MID NODE OF FIRST ELEMENT AND THEN CYCLE
C      THROUGH EACH ELEMENT.
C      DO 120 II = 1, NE
C      I = II
C      IF(NTE(II).EQ.2) GOTO500
C      IF(NTE(II).EQ.3) GOTO600
C      GOTO111
C
C      FIND HREL, WRL, AND TWEL AT LOC NODES 3,4,5(ROTOR).

```

```

STR09120
STR09130
STR09140
STR09150
STR09160
STR09170
STR09180
STR09190
STR09200
STR09210
STR09220
STR09230
STR09240
STR09250
STR09260
STR09270
STR09280
STR09290
STR09300
STR09310
STR09320
STR09330
STR09340
STR09350
STR09360
STR09370
STR09380
STR09390
STR09400
STR09410
STR09420
STR09430
STR09440
STR09450
STR09460
STR09470
STR09480
STR09490
STR09500
STR09510
STR09520
STR09530
STR09540
STR09550
STR09560
STR09570
STR09580
STR09590

```

AD-A038 759

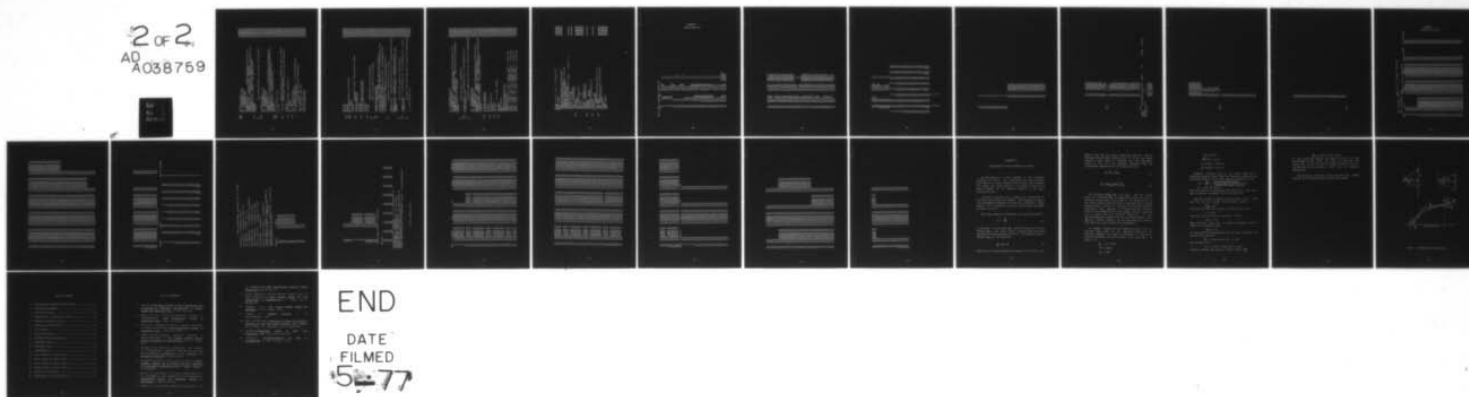
NAVAL POSTGRADUATE SCHOOL MONTEREY CALIF
THE FINITE ELEMENT METHOD APPLIED TO FLOWS IN TURBOMACHINES.(U)
DEC 76 V F GAVITO

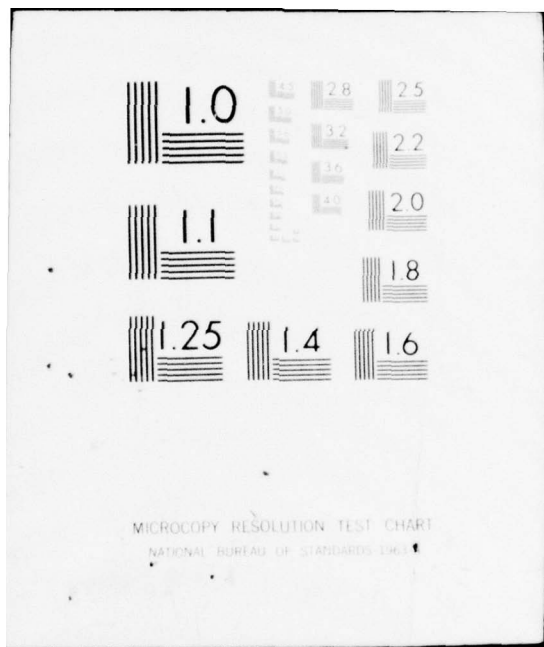
F/6 20/4

UNCLASSIFIED

NL

2 of 2
AD
A038759






```

500 DO 501 J = 3,5
502 VZ = UVEL(NODE(II,J))
VR = VVEL(NODE(II,J))
A = BE(NODE(II,J))
R = RC(NODE(II,J))
H(NODE(II,J)) = H(NODE(II,J)) - (WG*R)**2
H(NODE(II,J)) = H(NODE(II,J))/7.209035D06 + HS(NODE(II,J))
H(NODE(II,J)) = H(NODE(II,J)) + VZ*VZ)*DTAN(A)
TWEL(NODE(II,J)) = R*(WG*R - TWEL(NODE(II,J)))
WRL(NODE(II,J)) = R*(WG*R - TWEL(NODE(II,J)))
CONTINUE
GOTO111

501 FIND H,WRL,AND TVEL AT LOC NODES 3,4,5(STATOR).
C
C
C
600 DO 601 J = 3,5
VZ = UVEL(NODE(II,J))
VR = VVEL(NODE(II,J))
A = ALP(NODE(II,J))
R = RC(NODE(II,J))
H(NODE(II,J)) = H(NODE(II,J)) - (WG*R)**2
H(NODE(II,J)) = H(NODE(II,J))/7.209035D06 + HS(NODE(II,J))
H(NODE(II,J)) = H(NODE(II,J)) + VZ*VZ)*DTAN(A)
TWEL(NODE(II,J)) = R*(WG*R - TWEL(NODE(II,J)))
WRL(NODE(II,J)) = R*(WG*R - TWEL(NODE(II,J)))
CONTINUE
N = 2
P = PSI(NODE(II,N))
IT = 0
I = II
CHECK TO SEE IF P IS WITHIN THE PRESENT ELEMENT
IF(P-GE.PSI(NODE(I,5)))GOTO140
CHECK NEXT ELEMENT BELOW THE PRESENT ELEMENT.
I = I + 1
GOTO130
130 IF(P.GT.PSI(NODE(I,4)))GOTO170
C
140 EL = E1(4)
ER = E1(5)
E = (EL + ER)/2.D0
CALL SHAPE(E,-1.D0,SF)
PA = SF(3)*PSI(NODE(I,3)) + SF(4)*PSI(NODE(I,4))
1 + SF(5)*PSI(NODE(I,5))
CHECK FOR STREAMLINE CONVERGENCE
EPS = DABS(PA - P)
IF(EPS.LT.1.D-06)GOTO190
IT = IT + 1
IF(IT.GT.10)GOTO190
IF(PA.LT.P)GOTO160
C
150 STR09600
STR09610
STR09620
STR09630
STR09640
STR09650
STR09660
STR09670
STR09680
STR09690
STR09700
STR09710
STR09720
STR09730
STR09740
STR09750
STR09760
STR09770
STR09780
STR09790
STR09800
STR09810
STR09820
STR09830
STR09840
STR09850
STR09860
STR09870
STR09880
STR09890
STR09900
STR09910
STR09920
STR09930
STR09940
STR09950
STR09960
STR09970
STR09980
STR09990
STR10000
STR10010
STR10020
STR10030
STR10040
STR10050
STR10060
STR10070

```

```

160 EL = E
    GOTOL50
170 ER = E
    GOTOL50
165 IF(P.GT.PSI(NODE(I,3)))GOTO180
    EL = E1(3)
    ER = E1(4)
    GOTOL50
    CHECK NEXT ELEMENT ABOVE PRESENT ELEMENT
180 IF(KK.GT.0)GOTO185
    IF(I.EQ.1)GOTO165
    I = I - 1
    GOTOL40
185 IF(I.EQ.1.AND.N.EQ.2)GOTO187
    IF(I.EQ.1.AND.N.EQ.8)GOTO187
    I = I - 1
    GOTOL40
    I = I
    GOTOL65
    CONVERGENCE CRITERIA SATISFIED.
    CHECK TO SEE WHAT TYPE OF ELEMENT.
190 IF(NTE(II).EQ.3)GOTO195
    IF(NTE(II).EQ.2)GOTO196
    CALCULATE WHIRL AND STATIC ENTHALPY(DUCT)
    WRL(NODE(II,N)) = SF(3)*WRL(NODE(I,3)) + SF(4)*WRL(NODE(I,4))
    1 + SF(5)*WRL(NODE(I,5))
    HS(NODE(II,N)) = SF(3)*HS(NODE(I,3)) + SF(4)*HS(NODE(I,4))
    1 + SF(5)*HS(NODE(I,5))
    TVEL(NODE(II,N)) = WRL(NODE(II,N))/RC(NODE(II,N))
    CALCULATE TOT ENTHALPY AT THE NODE.
    H(NODE(II,N)) = UVEL(NODE(II,N))*2*(1.DO + DTAN(ALP(NODE(II,N))))*
    1*2)
    H(NODE(II,N)) = H(NODE(II,N)) + VVEL(NODE(II,N))*2
    H(NODE(II,N)) = HS(NODE(II,N)) + H(NODE(II,N))/7.20935D06
    GOTOL99
    CALCULATE TOT ENTHALPY AT NODE(STATOR).
    H(NODE(II,N)) = SF(3)*H(NODE(I,3)) + SF(4)*H(NODE(I,4)) + SF(5)*
    1 H(NODE(I,5))
    CALCULATE TVEL,SWHRL,AND STATIC ENTHALPY AT NODE(STATOR)
    VZ = UVEL(NODE(II,N))

```

```

STR10080
STR10090
STR10100
STR10110
STR10120
STR10130
STR10140
STR10150
STR10160
STR10170
STR10180
STR10190
STR10200
STR10210
STR10220
STR10230
STR10240
STR10250
STR10260
STR10270
STR10280
STR10290
STR10300
STR10310
STR10320
STR10330
STR10340
STR10350
STR10360
STR10370
STR10380
STR10390
STR10400
STR10410
STR10420
STR10430
STR10440
STR10450
STR10460
STR10470
STR10480
STR10490
STR10500
STR10510
STR10520
STR10530
STR10540
STR10550

```



```

SF(8) = (1.D0 - E*E + Z - Z*E*E)/2.D0
RETURN
DEBUG SUBCHK
END

SUBROUTINE M10T(RC,ZC,NODE,NN,NE)
IMPLICIT REAL*8(A-H,P-Z)
DIMENSION RC(NN),ZC(NN),OP1(9),OP2(9)
DIMENSION O1(107),O2(107)
DIMENSION NODE(NN,8)
REAL*8 TITLE(3),GAVITO,'NASA','TASK 1'
DATA OSCALE/.24/
DO 100 L = 1,NN
O1(L) = ZC(L)*OSCALE
O2(L) = RC(L)*OSCALE
CONTINUE
CALL PLOTS
CALL PLOT(0,0,3.0,-3)
DO 200 I = 1,NE
NPE = 9
DO 300 J = 1,8
OP1(J) = O1(NODE(I,J))
OP2(J) = O2(NODE(I,J))
CONTINUE
CP1(NPE) = OP1(1)
OP2(NPE) = OP2(1)
CALL LINE(OP1,OP2,NPE,1,1)
CONTINUE
DO 400 K = 1,NN
OL = FLOAT(K)
CALL NUMBER(O1(K),O2(K),.07,OL,0,-1)
CONTINUE
CALL SYMBOL(0.0,5.0,.14,TITLE,0.0,24)
CALL PLOT(0.0,7.0,-3)
CALL PLOT
RETURN
DEBUG SUBCHK
END

```

```

STR11040
STR11050
STR11060
STR11070
MPL00010

MPL00040
MPL00060

MPL00090
MPL00100
MPL00110
MPL00130
MPL00140
MPL00150

MPL00180

MPL00220

MPL00260
MPL00270
MPL00280
MPL00290
MPL00340
MPL00350
MPL00360

```


APPENDIX B SAMPLE INPUT DATA

NASA TASK-1	TRANSONIC	COMPRESSOR	
1C7	28		
1	0.00	18.878	1.
2	.00	17.439	1.
3	.00	16.0	1.
4	.00	14.5	1.
5	.00	13.0	1.
6	.00	11.5	1.
7	.00	10.0	1.
8	.00	8.5495	1.
9	.00	7.099	1.
10	.00	18.484	1.
11	.00	16.0	1.
12	.00	13.0	1.
13	.00	10.0	1.
14	.00	7.099	1.
15	.00	18.409	1.
16	.00	17.205	1.
17	.00	16.0	1.
18	.00	14.5	1.
19	.00	13.0	1.
20	.00	11.5	1.
21	.00	10.0	1.
22	.00	8.5495	1.
23	.00	7.099	1.
24	.00	18.403	1.
25	.00	15.798	1.
26	.00	12.897	1.
27	.00	9.996	1.
28	.00	7.145	1.
29	.00	18.397	1.
30	.00	16.996	1.
31	.00	15.595	1.
32	.00	14.194	1.
33	.00	12.794	1.
34	.00	11.393	1.
35	.00	9.992	1.
36	.00	8.591	1.
37	.00	7.19	1.
38	.00	18.37	1.
39	.00	15.835	1.
40	.00	13.3765	1.
41	.00	10.23	1.
42	.00	8.25	1.
43	.00	18.25	1.
44	.00	17.161	1.
45	.00	16.072	1.
46	.00	14.855	1.
			9921628
			.991016
			.989867
			.988101

47	18.256	13.638	.986334
48	18.192	12.659	.984340
49	18.128	11.658	.982346
50	18.064	10.403	.978950
51	18.522	9.125	.975553
52	19.524	18.037	.954283
53	19.527	16.037	.931421
54	19.528	13.706	.896215
55	19.53	11.778	.858371
56	20.533	9.634	.792201
57	20.599	17.871	.992424
58	20.665	17.937	.991146
59	20.731	16.002	.989867
60	20.797	14.888	.988100
61	20.862	13.773	.986336
62	20.928	12.824	.984242
63	20.994	11.875	.982148
64	21.06	11.009	.989852
65	21.692	10.142	.997555
66	21.802	17.838	1.
67	21.911	15.822	1.
68	22.031	14.286	1.
69	22.13	12.348	1.
70	22.85	10.336	.988014
71	22.904	17.711	.987362
72	22.958	16.586	.987650
73	22.962	15.589	.986970
74	23.028	14.859	.986091
75	23.062	14.132	.985934
76	23.096	13.415	.984777
77	23.148	12.698	.983765
78	23.2	11.625	.982754
79	23.225	10.553	.902611
80	24.615	17.836	.902895
81	24.610	15.642	.904722
82	24.605	14.228	.904722
83	24.6	12.852	.903892
84	24.64	10.831	.902994
85	26.336	17.836	.988014
86	26.273	16.767	.987362
87	26.232	15.697	.987650
88	26.191	15.011	.986970
89	26.152	14.325	.986091
90	26.113	13.665	.98543
91	26.056	13.005	.98477
92	26.0	12.057	.983762
93	26.7	11.109	.982754
94	29.	17.839	1.

102

8 9
10 11 12 13 14 15 16 17 18 19 20 21 22 23 24 25 26 27 28

1 1 1 1 1 2 2 2 2 1 1 1 1 3 3 3 3 1 1 1 1 3
43 44 45 46 47 48 49 50 51 52 53 54 55 56 57 58 59 60 61 62 63 64 65 66 67 68 69

755553
755379
755029
721694
688183
63146
574737
475777
376817
723788
703717
710175
670003
624479
692198
672301
652404
692372
732166
748921
765501
871094
871966
692198
652404
732166
75721

70 .871967
 71 .692198
 72 .672301
 73 .652404
 74 .692372
 75 .732166
 76 .740544
 77 .748921
 78 .810444
 79 .871967
 80 .346099
 81 .326202
 82 .36617
 83 .40300
 84 .435983

STOP

43 1.08
 44 1.0369
 45 .993791
 46 .950681
 47 .907571
 48 .881915
 49 .856259
 50 .823534
 51 .790809
 52 1.040565
 53 .967785
 54 .831475
 55 .707731
 56 .477173
 57 1.001121
 58 .97145
 59 .941605
 60 .848405
 61 .755204
 62 .657117
 63 .559029
 64 .361283
 65 .163537

107.6 STOP 201.482573318.846572 .08192 .08 15.0546 499.38
 4359.5
 53.35
 17.1250719 1.4

.240

1017.1250719
 1517.1250719
 2417.1250719
 2917.1250719

38	17	:	1250719	
43	17	:	1250719	
52	17	:	1250719	
57	17	:	1250719	
66	17	:	1250719	
71	17	:	1250719	
80	17	:	1250719	
85	17	:	1250719	
94	17	:	1250719	
14		:	0.0	
23		:	0.0	
28		:	0.0	
37		:	0.0	
42		:	0.0	
51		:	0.0	
56		:	0.0	
65		:	0.0	
70		:	0.0	
79		:	0.0	
84		:	0.0	
93		:	0.0	
98		:	0.0	
11				
12				
13				
16				
17				
18				
19				
20				
21				
22				
25				
26				
27				
30				
31				
32				
33				
34				
35				
36				
39				
40				
41				
44				
45				

STOP

46
47
48
49
50
53
54
55
58
59
60
61
62
63
64
67
68
69
72
73
74
75
76
77
78
81
82
83
86
87
88
89
90
91
92
95
96
97

STOP

APPENDIX C SAMPLE OUTPUT LISTING

NASA TASK-1 TRANSONIC COMPRESSOR									
NO. OF NODES = 107									
NODE	NO. OF ELEMENTS	Z(I)	SUMMARY OF NODAL COORDINATES		REL FLOW ANG	ABS FLOW ANG	REL FLOW ANG	ABS FLOW ANG	REL FLOW ANG
			R(I)	B(I)					
1		0.0	0.188780D	0.100000D	01	0.0	0.0	0.0	0.0
2		0.0	0.174390D	0.100000D	01	0.0	0.0	0.0	0.0
3		0.0	0.160000D	0.100000D	01	0.0	0.0	0.0	0.0
4		0.0	0.145000D	0.100000D	01	0.0	0.0	0.0	0.0
5		0.0	0.130000D	0.100000D	01	0.0	0.0	0.0	0.0
6		0.0	0.115000D	0.100000D	01	0.0	0.0	0.0	0.0
7		0.0	0.100000D	0.100000D	01	0.0	0.0	0.0	0.0
8		0.0	0.854950D	0.100000D	01	0.0	0.0	0.0	0.0
9		0.0	0.709900D	0.100000D	01	0.0	0.0	0.0	0.0
10		0.300000D	0.184840D	0.100000D	01	0.0	0.0	0.0	0.0
11		0.300000D	0.160000D	0.100000D	01	0.0	0.0	0.0	0.0
12		0.300000D	0.130000D	0.100000D	01	0.0	0.0	0.0	0.0
13		0.300000D	0.100000D	0.100000D	01	0.0	0.0	0.0	0.0
14		0.300000D	0.709900D	0.100000D	01	0.0	0.0	0.0	0.0
15		0.600000D	0.184090D	0.100000D	01	0.0	0.0	0.0	0.0
16		0.600000D	0.172050D	0.100000D	01	0.0	0.0	0.0	0.0
17		0.600000D	0.160000D	0.100000D	01	0.0	0.0	0.0	0.0
18		0.600000D	0.145000D	0.100000D	01	0.0	0.0	0.0	0.0
19		0.600000D	0.130000D	0.100000D	01	0.0	0.0	0.0	0.0
20		0.600000D	0.115000D	0.100000D	01	0.0	0.0	0.0	0.0
21		0.600000D	0.100000D	0.100000D	01	0.0	0.0	0.0	0.0
22		0.600000D	0.854950D	0.100000D	01	0.0	0.0	0.0	0.0
23		0.600000D	0.709900D	0.100000D	01	0.0	0.0	0.0	0.0
24		0.890200D	0.184030D	0.100000D	01	0.0	0.0	0.0	0.0
25		0.890200D	0.157980D	0.100000D	01	0.0	0.0	0.0	0.0
26		0.890200D	0.128970D	0.100000D	01	0.0	0.0	0.0	0.0
27		0.890200D	0.999600D	0.100000D	01	0.0	0.0	0.0	0.0
28		0.890200D	0.714500D	0.100000D	01	0.0	0.0	0.0	0.0
29		0.118040D	0.183970D	0.100000D	01	0.0	0.0	0.0	0.0
30		0.118040D	0.169960D	0.100000D	01	0.0	0.0	0.0	0.0
31		0.118040D	0.155950D	0.100000D	01	0.0	0.0	0.0	0.0
32		0.118040D	0.141940D	0.100000D	01	0.0	0.0	0.0	0.0
33		0.118040D	0.127940D	0.100000D	01	0.0	0.0	0.0	0.0
34		0.118040D	0.113930D	0.100000D	01	0.0	0.0	0.0	0.0
35		0.118040D	0.999200D	0.100000D	01	0.0	0.0	0.0	0.0
36		0.118040D	0.859100D	0.100000D	01	0.0	0.0	0.0	0.0
37		0.118040D	0.719000D	0.100000D	01	0.0	0.0	0.0	0.0
38		0.155000D	0.183700D	0.100000D	01	0.0	0.0	0.0	0.0
39		0.155000D	0.158350D	0.100000D	01	0.0	0.0	0.0	0.0
40		0.155000D	0.133000D	0.100000D	01	0.0	0.0	0.0	0.0
41		0.155000D	0.107650D	0.100000D	01	0.0	0.0	0.0	0.0
42		0.155000D	0.823000D	0.100000D	01	0.0	0.0	0.0	0.0

43	0.	1851100	02	0.	1825000	02	0.	992163D	00	0.	7555530	00	0.	1080000	01
44	0.	1844700	02	0.	1716100	02	0.	9910160	00	0.	7553790	00	0.	1036900	01
45	C.	1838300	02	0.	1607200	02	0.	9898670	00	0.	7550290	00	0.	9937910	00
46	0.	1831900	02	0.	1485500	02	0.	9881010	00	0.	7216940	00	0.	9506810	00
47	0.	1825600	02	0.	1363800	02	0.	9863340	00	0.	6818300	00	0.	9075710	00
48	0.	1819200	02	0.	1265900	02	0.	9843400	00	0.	6314600	00	0.	8819150	00
49	0.	1812800	02	0.	1168000	02	0.	9823460	00	0.	5747370	00	0.	8562590	00
50	0.	1806400	02	0.	1040300	02	0.	9789500	00	0.	4757770	00	0.	8235340	00
51	0.	1800000	02	0.	9125000	01	0.	9755530	00	0.	3768170	00	0.	7908090	00
52	0.	1952200	02	0.	1801000	02	0.	9542830	00	0.	7237880	00	0.	1040570	01
53	0.	1952400	02	0.	1603700	02	0.	9314210	00	0.	7037170	00	0.	9677850	00
54	0.	1952700	02	0.	1370600	02	0.	8962150	00	0.	7101750	00	0.	8314750	00
55	C.	1952800	02	0.	1177800	02	0.	8583710	00	0.	6700030	00	0.	7077310	00
56	0.	1953000	02	0.	9634000	01	0.	7922010	00	0.	6244790	00	0.	4771730	00
57	0.	2053300	02	0.	1787100	02	0.	9924240	00	0.	6921980	00	0.	1001120	01
58	0.	2059900	02	0.	1693700	02	0.	9911450	00	0.	6723010	00	0.	9714500	00
59	0.	2066500	02	0.	1600200	02	0.	9898670	00	0.	6524040	00	0.	9416050	00
60	0.	2073100	02	0.	1488800	02	0.	9881000	00	0.	6923720	00	0.	8484050	00
61	0.	2079700	02	0.	1377300	02	0.	9863360	00	0.	7321660	00	0.	7552040	00
62	0.	2086200	02	0.	1282400	02	0.	9842420	00	0.	7489210	00	0.	6571170	00
63	0.	2092800	02	0.	1187500	02	0.	9821480	00	0.	7655010	00	0.	5590290	00
64	0.	2099400	02	0.	1100900	02	0.	9898520	00	0.	8710940	00	0.	3612830	00
65	0.	2106000	02	0.	1014200	02	0.	9975550	00	0.	8719660	00	0.	1635370	00
66	0.	2169200	02	0.	1783800	02	0.	1000000	01	0.	6921980	00	0.	0.	0.
67	0.	2180200	02	0.	1582200	02	0.	1000000	01	0.	6524040	00	0.	0.	0.
68	0.	2191100	02	0.	1400000	02	0.	1000000	01	0.	7321660	00	0.	0.	0.
69	0.	2213000	02	0.	1286000	02	0.	1000000	01	0.	7572100	00	0.	0.	0.
70	0.	2285000	02	0.	1034800	02	0.	1000000	01	0.	8719670	00	0.	0.	0.
71	0.	2290400	02	0.	1671100	02	0.	9880140	00	0.	6921980	00	0.	0.	0.
72	0.	2295800	02	0.	1558600	02	0.	9873620	00	0.	6723010	00	0.	0.	0.
73	0.	2296200	02	0.	1485900	02	0.	9869700	00	0.	6524040	00	0.	0.	0.
74	0.	2302800	02	0.	1413200	02	0.	9860910	00	0.	7321660	00	0.	0.	0.
75	0.	2306200	02	0.	1341500	02	0.	9859340	00	0.	7405440	00	0.	0.	0.
76	0.	2309600	02	0.	1269800	02	0.	9847770	00	0.	7489210	00	0.	0.	0.
77	0.	2314800	02	0.	1162500	02	0.	9837650	00	0.	8104440	00	0.	0.	0.
78	0.	2320000	02	0.	1055300	02	0.	9827540	00	0.	8719670	00	0.	0.	0.
79	0.	2462500	02	0.	1783600	02	0.	9026110	00	0.	3460990	00	0.	0.	0.
80	0.	2461500	02	0.	1564200	02	0.	9028950	00	0.	3262020	00	0.	0.	0.
81	0.	2461000	02	0.	1422800	02	0.	9047250	00	0.	3661700	00	0.	0.	0.
82	0.	2460500	02	0.	1285200	02	0.	9038920	00	0.	4030000	00	0.	0.	0.
83	0.	2460000	02	0.	1083100	02	0.	9029940	00	0.	0.	0.	0.	0.	0.
84	0.	2640000	02	0.	1783600	02	0.	9880140	00	0.	0.	0.	0.	0.	0.
85	0.	2633600	02	0.	1676700	02	0.	9873620	00	0.	0.	0.	0.	0.	0.
86	0.	2627300	02	0.	1569700	02	0.	9876500	00	0.	0.	0.	0.	0.	0.
87	0.	2623200	02	0.	1501100	02	0.	9869700	00	0.	0.	0.	0.	0.	0.
88	0.	2619100	02	0.	1432500	02	0.	9860910	00	0.	0.	0.	0.	0.	0.
89	0.	2615200	02	0.	1366500	02	0.	9854300	00	0.	0.	0.	0.	0.	0.

INLET THERMODYNAMIC VARIABLES ARE AS FOLLOWS

FLOW RATE = 0.107600D 03 LBM/SEC
 TOT DENSITY = 0.819200D-01 LBM CU FT
 TOT PRESSURE = 0.150546 D 02 PSI
 TOT TEMPERATURE = 0.499380D 03 DEG RANKINE
 ROTATIONAL SPEED = 0.435950D 04 RPM
 INLET U VELOCITY = 0.201483D 03 FT/SEC
 OUTLET U VELOCITY = 0.318847D 03 FT/SEC
 GAS CONSTANT = 0.533500D 02
 RATIO OF SPECIFIC HEATS = 0.140000D 01
 SPECIFIC HEAT AT CONSTANT PRESSURE = 0.240000D 00
 STATIC DENSITY AT INLET = 0.800000D-01
 INITIAL ESTIMATE OF PSI DISTRIBUTION = 0.171251D 02
 NODES WHERE PSI IS SPECIFIED

NODE NO.	PSI (11)
10	0.171251D 02
15	0.171251D 02
24	0.171251D 02
29	0.171251D 02
38	0.171251D 02
43	0.171251D 02
52	0.171251D 02
57	0.171251D 02
66	0.171251D 02
71	0.171251D 02
80	0.171251D 02
85	0.171251D 02
94	0.171251D 02
14	0.0
23	0.0
28	0.0
37	0.0
42	0.0
51	0.0
56	0.0

```

65 0.0
70 0.0
79 0.0
84 0.0
93 0.0
98 0.0
1 0.171251D 02
2 0.142002D 02
3 0.115071D 02
4 0.894662D 01
5 0.663797D 01
6 0.458117D 01
7 0.277622D 01
8 0.127036D 01
9 0.0
99 0.171251D 02
100 0.145999D 02
101 0.121933D 02
102 0.981814D 01
103 0.757093D 01
104 0.545171D 01
105 0.346047D 01
106 0.167140D 01
107 0.0

```

NODES WHERE F(R,Z) IS SPECIFIED

NODE NO.	11	12	13	16	17	18	19	20	21
11	12	13	16	17	18	19	20	21	21
22	25	26	27	30	31	32	33	34	34
35	36	39	40	41	44	45	46	47	47
48	49	50	53	54	55	58	59	60	60
61	62	63	64	67	68	69	72	73	73
74	75	76	77	78	81	82	83	86	86
87	88	89	90	91	92	95	96	97	97

LARGEST EPS FOR ITERATION 1 IS 0.136047897529D 02
ITERATION NO. 1 COMPLETE
STREAM FUNCTION CONVERGENCE NOT YET SATISFIED.
NEXT ITERATION IS IN PROGRESS
LARGEST EPS FOR ITERATION 2 IS 0.442913378700D 00
PROGRAM TERMINATED ON ITERATION NO. 2
RESULTS WHICH FOLLOW ARE FOR CONVERGENCE EPSILON = 0.442913378700D 00

FINITE ELEMENT RESULTS

NODE	PSI(I)	VZ	VR	R(I)	DENSITY
1	0.171251D 02	0.201483D 03	0.0	0.188780D 02	0.800000D-01
2	0.142002D 02	0.201483D 03	0.0	0.174390D 02	0.800000D-01
3	0.115071D 02	0.201483D 03	0.0	0.160000D 02	0.800000D-01
4	0.894662D 01	0.201483D 03	0.0	0.145000D 02	0.800000D-01
5	0.663797D 01	0.201483D 03	0.0	0.130000D 02	0.800000D-01
6	0.458117D 01	0.201483D 03	0.0	0.115000D 02	0.800000D-01
7	0.277622D 01	0.201483D 03	0.0	0.100000D 02	0.800000D-01
8	0.127036D 01	0.201483D 03	0.0	0.854950D 01	0.800000D-01
9	0.0	0.201483D 03	0.0	0.709900D 01	0.800000D-01
10	0.171251D 02	0.220059D 03	-0.172013D 02	0.184840D 02	0.802734D-01
11	0.118445D 02	0.210036D 03	-0.14073D 02	0.160000D 02	0.804297D-01
12	0.678256D 01	0.206122D 03	-0.730155D 01	0.130000D 02	0.804687D-01
13	0.282503D 01	0.202621D 03	-0.272330D 01	0.100000D 02	0.805078D-01
14	0.0	0.205347D 03	0.0	0.709900D 01	0.804883D-01
15	0.171251D 02	0.211902D 03	-0.438116D 00	0.184090D 02	0.803906D-01
16	0.145630D 02	0.216573D 03	0.465115D 01	0.172050D 02	0.803125D-01
17	0.121188D 02	0.216545D 03	-0.158781D 01	0.160000D 02	0.803125D-01
18	0.937887D 01	0.212585D 03	-0.679883D 01	0.145000D 02	0.803906D-01
19	0.695622D 01	0.213867D 03	-0.684264D 01	0.130000D 02	0.803516D-01
20	0.477052D 01	0.212284D 03	-0.673067D 01	0.115000D 02	0.803906D-01
21	0.286757D 01	0.204643D 03	-0.564721D 01	0.100000D 02	0.805078D-01
22	0.132090D 01	0.206900D 03	0.225277D 01	0.854950D 01	0.804687D-01
23	0.0	0.210041D 03	0.336558D 01	0.709900D 01	0.804297D-01
24	0.171251D 02	0.227675D 03	-0.470728D 00	0.184030D 02	0.801562D-01
25	0.119735D 02	0.205688D 03	-0.166029D 02	0.157980D 02	0.804687D-01
26	0.702133D 01	0.220263D 03	-0.148156D 02	0.128970D 02	0.802539D-01
27	0.292664D 01	0.226396D 03	-0.223632D 01	0.999600D 02	0.801953D-01
28	0.0	0.198306D 03	0.310921D 01	0.714500D 01	0.805664D-01
29	0.171251D 02	0.226429D 03	-0.109332D 01	0.183970D 02	0.801758D-01
30	0.142776D 02	0.183610D 03	-0.795651D 02	0.169960D 02	0.805469D-01
31	0.122341D 02	0.206530D 03	-0.166455D 03	0.155950D 02	0.795312D-01
32	0.974105D 01	0.228187D 03	-0.172725D 03	0.141940D 02	0.791406D-01
33	0.724815D 01	0.241888D 03	-0.179660D 03	0.127940D 02	0.788672D-01
34	0.498124D 01	0.245654D 03	-0.130826D 03	0.113930D 02	0.792969D-01
35	0.292974D 01	0.245873D 03	-0.662508D 02	0.999200D 01	0.797266D-01
36	0.124448D 01	0.218274D 03	-0.183315D 02	0.859100D 01	0.802930D-01
37	0.0	0.181316D 03	-0.469758D 02	0.719000D 01	0.807422D-01
38	0.171251D 02	0.953714D 02	-0.209029D 01	0.183700D 02	0.816016D-01
39	0.156118D 02	0.211283D 03	0.488500D-01	0.158350D 02	0.803906D-01
40	0.107447D 02	0.341329D 03	0.124478D 02	0.133000D 02	0.780078D-01
41	0.467601D 01	0.359152D 03	0.419968D 02	0.107650D 02	0.775391D-01
42	0.0	0.365127D 03	0.114029D 03	0.823000D 01	0.770312D-01
43	0.171251D 02	0.188915D 03	-0.542827D 02	0.182500D 02	0.836719D-01
44	0.150236D 02	0.182983D 03	-0.363786D 02	0.171610D 02	0.840625D-01
45	0.131222D 02	0.181377D 03	-0.358019D 02	0.160720D 02	0.835156D-01

46	0.109989D	02	0.217508D	03	-0.332291D	02	0.148555D	02	0.804687D	-01
47	0.874510D	01	0.263002D	03	-0.321793D	02	0.136380D	02	0.771484D	-01
48	0.684972D	01	0.300928D	03	-0.128776D	02	0.126590D	02	0.751172D	-01
49	0.490441D	01	0.357638D	03	0.801256D	01	0.116800D	02	0.718555D	-01
50	0.237289D	01	0.385140D	03	0.629724D	02	0.104030D	02	0.710547D	-01
51	0.0	01	0.433195D	03	0.144257D	03	0.912500D	01	0.681250D	-01
52	0.171251D	02	0.242434D	03	-0.454414D	02	0.160100D	02	0.800000D	-01
53	0.132234D	02	0.208945D	03	0.543397D	01	0.180370D	02	0.826172D	-01
54	0.883947D	01	0.334585D	03	0.477602D	02	0.137060D	02	0.726172D	-01
55	0.476760D	01	0.538251D	03	0.107145D	03	0.117780D	02	0.600391D	-01
56	0.0	01	0.684311D	03	0.227433D	03	0.963400D	01	0.600391D	-01
57	0.171251D	02	0.281327D	03	-0.117674D	02	0.178710D	02	0.800000D	-01
58	0.147764D	02	0.236773D	03	0.134070D	02	0.169370D	02	0.817578D	-01
59	0.128904D	02	0.217194D	03	0.529913D	02	0.160020D	02	0.825391D	-01
60	0.106224D	02	0.252037D	03	0.812332D	02	0.148880D	02	0.789453D	-01
61	0.827315D	01	0.303197D	03	0.114025D	03	0.137730D	02	0.743359D	-01
62	0.619073D	01	0.341721D	03	0.132514D	03	0.128240D	02	0.717969D	-01
63	0.408225D	01	0.401864D	03	0.150547D	03	0.118750D	02	0.681836D	-01
64	0.207387D	01	0.491840D	03	0.147459D	03	0.110090D	02	0.618750D	-01
65	0.0	01	0.567354D	03	0.109494D	03	0.101420D	02	0.600391D	-01
66	0.171251D	02	0.302506D	03	0.456957D	01	0.178380D	02	0.767383D	-01
67	0.120681D	02	0.255341D	03	-0.349385D	02	0.158220D	02	0.783984D	-01
68	0.798850D	01	0.300666D	03	0.802308D	02	0.140000D	02	0.762500D	-01
69	0.417127D	01	0.334517D	03	0.980101D	02	0.122860D	02	0.745703D	-01
70	0.0	01	0.445955D	03	0.856484D	02	0.103480D	02	0.662695D	-01
71	0.171251D	02	0.301848D	03	0.307300D	-12	0.178360D	02	0.767578D	-01
72	0.140702D	02	0.292879D	03	0.105376D	02	0.167110D	02	0.772070D	-01
73	0.112853D	02	0.299853D	03	0.288777D	02	0.155860D	02	0.771094D	-01
74	0.950536D	01	0.310703D	03	0.432739D	02	0.148590D	02	0.764062D	-01
75	0.774640D	01	0.328817D	03	0.559861D	02	0.141320D	02	0.753125D	-01
76	0.606420D	01	0.326266D	03	0.632255D	02	0.134150D	02	0.752734D	-01
77	0.448194D	01	0.328199D	03	0.724202D	02	0.126980D	02	0.750781D	-01
78	0.220067D	01	0.357466D	03	0.758258D	02	0.116250D	02	0.728516D	-01
79	0.0	01	0.401487D	03	0.797238D	02	0.105530D	02	0.690625D	-01
80	0.171251D	02	0.338282D	03	0.0	02	0.178360D	02	0.775781D	-01
81	0.110657D	02	0.357678D	03	0.267016D	02	0.156420D	02	0.771094D	-01
82	0.742061D	01	0.358663D	03	0.434724D	02	0.142280D	02	0.769141D	-01
83	0.420615D	01	0.347499D	03	0.534363D	02	0.128520D	02	0.770312D	-01
84	0.0	01	0.390797D	03	0.776011D	02	0.108310D	02	0.755273D	-01
85	0.171251D	02	0.312169D	03	0.567579D	00	0.178360D	02	0.786328D	-01
86	0.139682D	02	0.316128D	03	-0.126945D	03	0.167670D	02	0.780078D	-01
87	0.109162D	02	0.335360D	03	-0.277874D	03	0.156970D	02	0.755859D	-01
88	0.902395D	01	0.324992D	03	-0.331898D	03	0.150110D	02	0.747656D	-01
89	0.727694D	01	0.322973D	03	-0.392948D	03	0.143250D	02	0.733594D	-01
90	0.567134D	01	0.320579D	03	-0.356204D	03	0.136650D	02	0.743164D	-01
91	0.414305D	01	0.319875D	03	-0.318186D	03	0.130050D	02	0.751562D	-01
92	0.203268D	01	0.333436D	03	-0.163312D	03	0.120570D	02	0.773047D	-01
93	0.0	01	0.357598D	03	0.321838D	01	0.111090D	02	0.776172D	-01

115

82	0.244303D 05	0.124673D 03	0.143088D 03	0.0
83	0.265507D 05	0.127365D 03	0.172157D 03	0.0
84	0.326492D 05	0.134132D 03	0.251202D 03	0.0
85	0.0	0.119987D 03	0.0	0.0
86	0.0	0.120783D 03	0.0	0.0
87	0.0	0.122067D 03	0.0	0.0
88	0.0	0.123223D 03	0.0	0.0
89	0.0	0.124821D 03	0.0	0.0
90	0.0	0.126075D 03	0.0	0.0
91	0.0	0.127436D 03	0.0	0.0
92	0.0	0.130339D 03	0.0	0.0
93	0.0	0.134132D 03	0.0	0.0
94	0.0	0.120279D 03	0.0	0.0
95	0.0	0.122120D 03	0.0	0.0
96	0.0	0.125018D 03	0.0	0.0
97	0.0	0.127731D 03	0.0	0.0
98	0.0	0.132648D 03	0.0	0.0
99	0.0	0.120854D 03	0.0	0.0
100	0.0	0.121376D 03	0.0	0.0
101	0.0	0.122195D 03	0.0	0.0
102	0.0	0.123484D 03	0.0	0.0
103	0.0	0.125192D 03	0.0	0.0
104	0.0	0.126543D 03	0.0	0.0
105	0.0	0.128131D 03	0.0	0.0
106	0.0	0.129812D 03	0.0	0.0
107	0.0	0.131572D 03	0.0	0.0

APPENDIX D

CALCULATION OF ROTOR ELEMENT FLOW ANGLES

The following is a brief synopsis of the procedure contained in Ref.13 for calculating the outlet relative flow angles in a rotor element from the given inlet relative flow angle and blade solidity. The reader is referred to Ref.13, Chapter VI, for specific details of low speed correlation data.

As stated in Section III.A, uniform flow conditions at the rotor blade edges were assumed. This assumption coupled with knowledge of the mass flow rate and rotational speed, enables one to calculate the inlet relative flow angle, β_1 , as shown in Fig 18.

From blade geometry information, the blade solidity, σ ,

$$\sigma = \frac{c}{s} \quad (1)$$

is obtained. At this point, β_1 , and σ are given and one may calculate β_2 , the rotor outlet relative flow angle from correlation curves depicted in Ref 13. The equation used to determine β_2 , is the following,

$$\beta_2 = K_2 + \delta \quad (2)$$

where K_2 is the angle between the tangent to the blade mean

camber line and the axial direction (Fig 18). This is obtained from the blade geometry data. δ is the low speed deviation angle which is obtained from the correlation curves in Ref. 13. The following equations show the relationship between δ and the correlation data.

$$\delta = \delta_o + m\phi \quad (3)$$

$$\delta_o = (K\delta)_{sh} (K\delta)_t (\delta_o)_{io} \quad (4)$$

The variables $m, (K\delta)_{sh}, (K\delta)_t$ and $(\delta_o)_{io}$, are all values which are obtained from the correlation curves and are all functions of the given blade geometry. The quantity, ϕ , is the blade camber angle and again is obtained from the blade geometry data. Once all the variables are obtained from the correlation data, equation (4) is solved for the deviation angle for an uncambered blade section, δ_o , and then equation (3) is solved for the deviation angle, δ . One now calculates β_2 from equation (2) for the blade element. With β_2 now a known quantity, one now calculates the absolute flow angle, α_1 , from uniform flow assumptions.

An example follows for node numbers 43 and 57 (Fig 6). From Ref. [12], Table II, the following quantities are obtained assuming the angle of incidence, i , (Fig 18) is zero and therefore the inlet relative flow angle, β_1 , is equal to k_1 .

$$\beta_1 = k_1 = 61.88^\circ$$

$$r = 1.3062$$

$$\phi = 6.95^\circ$$

$$K_2 = 54.93^\circ$$

$$\frac{t}{c})_{\max} = 0.035$$

$$\text{tip radius} = 18.25 \text{ in}$$

$$\text{hub radius} = 9.125 \text{ in}$$

Assuming uniform flow at the rotor inlet and a rotational speed of 4359.5 RPM, the following quantities are determined from the rotor inlet velocity diagram (Fig 18).

$$V_m = \frac{\dot{m}}{\rho A} = \frac{(107.6 \text{ lbm/sec})(144 \text{ in}^2/\text{ft}^2)}{(0.08 \text{ lbm/ft}^3) \pi (18.25^2 - 9.125^2) \text{ in}^2}$$

$$V_m = 246.802 \text{ ft/sec}$$

where the area A, is determined from the hub and tip radii and the density is assumed to be 0.08 lbm/cu ft.

Now one is ready to obtain the correlation data. From Ref.[13], Fig 162, with $\beta_1 = 61.88^\circ$ and $\Gamma = 1.3062$,

$$\delta_o)_{\omega} = 2.50^\circ$$

From Ref.[13], Fig 162, with $\beta_1 = 61.88^\circ$ and $\Gamma = 1.3062$,

$$m = 0.235$$

From Ref.[13], Fig 172, with $t/c)_{\max} = 0.0350$,

$$k\delta)t = 0.29$$

From Ref.[13], page 222, one uses the following value of $(K\delta)_{sh}$ for 65-series blades,

$$(K\delta)_{sh} = 1.0$$

At this point all the necessary data has been obtained for equations (3) and (4),

$$\delta_o^\circ = (1.0)(0.29)(2.50) = 0.725^\circ$$

From equation (3),

$$\delta = 0.725^\circ + 0.235(6.95) = 2.36^\circ$$

Finally, equation (2) gives the desired value of β_2 ,

$$\beta_2 = 54.93^\circ + 2.36^\circ = 57.29^\circ$$

At this point the relative flow angle for node 57 has been obtained, $\beta_2 = 57.29^\circ$. These two values of relative flow angles, $\beta_1 = 61.88^\circ$ for node 43 and $\beta_2 = 57.29^\circ$ for node 57, are then read in the program as input data for numerical computation.

This process is repeated at each required blade element section for the proper outlet relative flow angle.

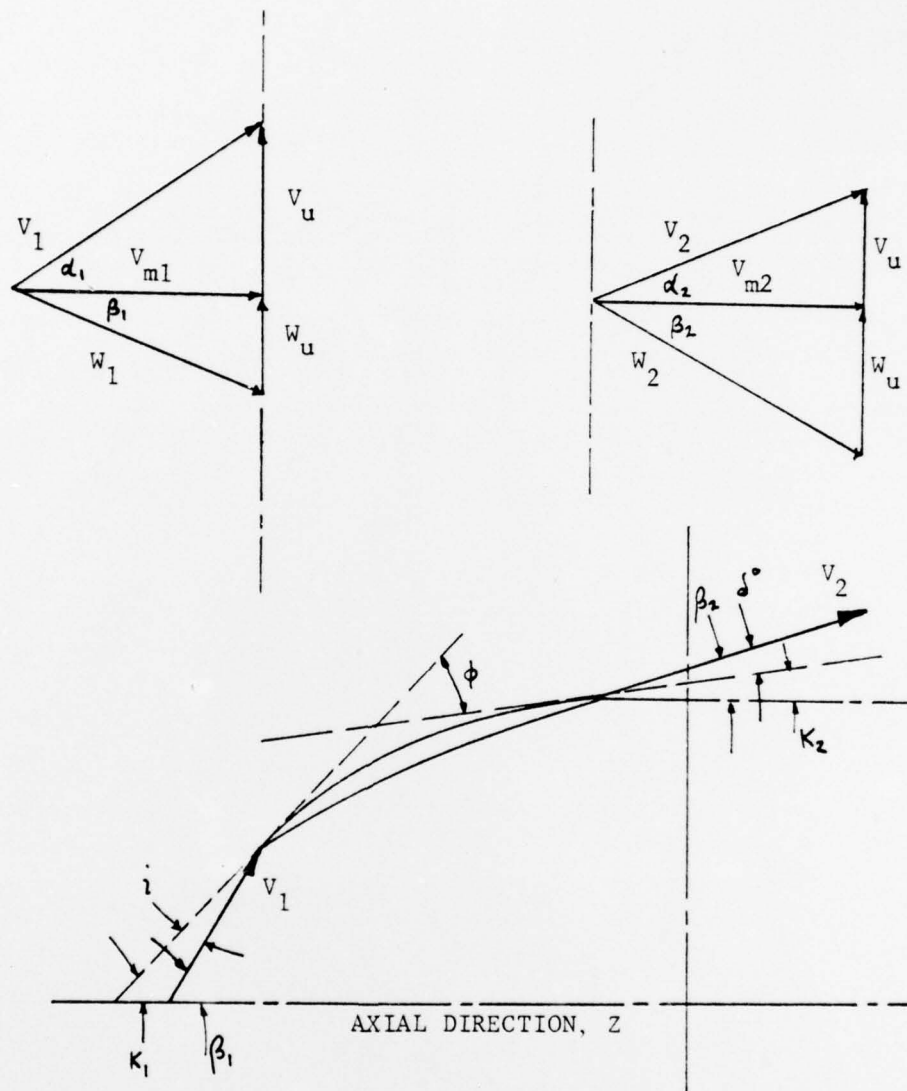


Figure 18 - NOMENCLATURE FOR CASCADE BLADE

LIST OF FIGURES

1. Meridional and Blade-to-Blade Planes.....	9
2. Turbomachine Geometry.....	11
3. Meridional Plane.....	18
4. Isoparametric quadrilateral Element.....	26
5. Gaussian Integration Points.....	31
6. Compressor Discretization.....	33
7. Duct Element.....	35
8. Program Flowchart.....	42
9. Stiffness Matrix Evaluation.....	51
10. SUBROUTINE SLINE.....	57
11. SUBROUTINE FCAL.....	60
12. SUBROUTINE VEL.....	65
13. Axial Profile at Rotor Inlet.....	71
14. Axial Profile at Rotor Outlet.....	72
15. Axial Profile at Stator Inlet.....	73
16. Axial Profile at Stator Outlet.....	74
17. Epsilon vs. Iterations.....	75
18. Nomenclature for Cascade Blade.....	121

LIST OF REFERENCES

1. NACA TN 2604, A General Theory of Three Dimensional Flow in Subsonic and Supersonic Turbomachines of Axial-, Radial, and Mixed-Flow Type, by C.H. Wu, 1952.
2. Smith, L.H., Jr., 'The Radial Equilibrium Equation of Turbomachinery', ASME Transactions, Journal of Engineering Power, v.88A, p.1-12, 1966.
3. Novak, R.A., 'Streamline Curvature Computing Procedures for Fluid Flow Problems', ASME Transactions, Journal of Engineering Power, v.89A, p.478, 1967.
4. REPORT ME/A-71-5, Carleton University, Division of Aerothermodynamics, A New Computer Program for the Design and Analysis of Turbomachinery, by W.R. Davis, 1971.
5. Wilkinson, D.H., 'Stability, Convergence, and Accuracy of Two-Dimensional Streamline Curvature Methods using Quasi-Orthogonals', Proceedings of the Institute of Mechanical Engineers, v.184, p.108, 1970.
6. Aeronautical Research Council, R and M 3509, A Digital Computer Program for the Through Flow Fluid Mechanics in an Arbitrary Turbomachine using a Matrix Method, by H. Marsh, 1966.
7. Hirsch, CH. and Warzee, G., 'A Finite Element Method for the Axisymmetric Flow Computation in a Turbomachine', International Journal for Numerical Methods in Engineering, v.10, p.93-113, 1976.
8. Horlock, J.H., 'On Entropy Production in Adiabatic Flow

in Turbomachines', ASME Transactions, Journal of Basic Engineering, v.930, p.587, 1971.

9. Report VUB-STR-5, Vrije Universiteit Brussel, Dept. of Fluid Mechanics, 'A Finite Element Method for Flow Calculations in Turbomachines, by C. Hirsch and G. Warzee, 1974.
10. Huebner, K.H., The Finite Element Method for Engineers, p. 117, Wiley, 1975.
11. Kaplan, W., Advanced Calculus, p. 93, Addison-Wesley, 1952.
12. NASA CR-72806, Vol I., Evaluation of Range and Distortion Tolerance for High Mach Number Transonic Free Stages, by C.C. Koch, K.R. Bilwakesh, and V.L. Doyle, 1971.
13. NASA-SP-36, Aerodynamic Design of Axial Flow Compressors, NASA staff, chap. VI-VII, 1965.
14. Vavra, M.H., Aero-Thermodynamics and Flow in Turbomachines, p. 308, Krieger, 1974.